

Maximizing Regenerative Braking Energy in Railway Vehicle of Addis Ababa



Yared Tadesse

Addis Ababa Institute of Technology

Addis Ababa University

Supervisor

Dr. Mengesha Mamo

A Thesis Submitted to
The School of Electrical and Computer Engineering

Presented in Fulfillment of The Requirements for The Degree of
Master of Science in Control Engineering

Addis Ababa, Ethiopia

December 19, 2017 GC

Certification

This is to certify that the thesis prepared by Yared Tadesse, entitled: *Maximizing regenerative braking energy in railway vehicle of Addis Ababa* and submitted in partial fulfillment of the requirements for the degree of Master Sciences in Control Engineering complies with the regulations of university and meets the accepted standards with respect to originality and quality.

Approved by board of examiners.

Dr Mengesha Mamo		
_____	_____	_____
Thesis Advisor	Signature	Date

Dr Dereje Shiferaw		
_____	_____	_____
Examiner	Signature	Date

Mr. Mihretab Negash		
_____	_____	_____
Examiner	Signature	Date

School Chair Person
Dr. Yalemzewd Negash

Declaration

This thesis is a presentation of my original research work. Where ever contribution of others are involved, every effort is made to indicate this clearly, with proper citation of sources. I, the under signed, declare the thesis has not been presented for degree in any other university.

Yared Tadesse

Acknowledgment

First, I would like to thank my GOD for every thing. I am very grateful to my advisor Dr. Mengesha Mamo for his positive feedbacks, supports and motivation. Next, I am thankful to my families, *good friends* and colleague Kinde Mekuria for their undeniable comments and motivation. Finally, I would like to thank all those open source code providers for laying the foundation in implementing optimization algorithm.

Abstract

In this thesis, the problem of maximizing regenerative braking energy is addressed to reduce electrical power consumption of Addis Ababa Light Rail Transit vehicle. The problem is solved using Improved Artificial Bee Colony(IABC) algorithm in case of Ayat-2 to Ayat-1, Mazoria to Chemical Corporation and Meskel Square-1 to Legehar stations and vice versa. The rail road has relatively smaller gradient from Ayat-2 to Ayat-1 station while steepest slope exist between Meskel Square-1 and Legehar station. After several simulation tests, the optimal regenerative braking speed profile that satisfies different constraints is recommended for aforementioned stations. As seen from the simulation results, the optimized braking can restore 25.6383% to 29.4083% total kinetic energy of vehicle in case of Meskel Square-1 to Legehar (2.767° gradient) and Ayat-2 to Ayat-1 (0.00905° gradient) uphill drive braking respectively. In recommended optimal regenerative braking operation, significant amount of electrical energy is restored as compared to constant braking rate operation. Particularly, $1.1984MJ$ electrical energy is regenerated using proposed method while $0.6115MJ$ is recovered using constant braking rate in case of Meskel Square-1 to Legehar uphill drive braking. In downhill drive braking operation, an increase in regenerative braking energy is observed since the tangential component of gravitational force exerted on the vehicle acts in direction of velocity. Numerically, $3.3669MJ$ energy is regenerated using IABC algorithm while $3.1074MJ$ energy is restored by constant braking rate operation in case of -2.767° gradient downhill drive braking.

Key words: Regenerative braking; Artificial bee colony algorithm; Addis Ababa light train;

List of Figures

2.1	Rail gauge types [1]	12
2.2	Curve resistance [2]	13
2.3	Grade or gradient resistance of train	16
2.4	Wheel-rail adhesion	17
2.5	Frictional force of sliding block	18
2.6	Normal force of railway vehicle on inclined surface	18
2.7	Available tractive effort as function of speed [3]	21
2.8	Braking speed vs distance for sequential computing [4]	22
3.1	Adhesive force vs speed on level railroad	38
3.2	AALRT vehicle running resistance vs speed	40
3.3	The tractive effort of AALRT vehicle with adhesion limit on level rail	41
3.4	Operating range of regenerative braking on level rail	42
4.1	Recommended RGB speed profile from Ayat-2 to Ayat-1	44
4.2	Recommended RGB speed profile from Ayat-1 to Ayat-2	45
4.3	Recommended RGB speed profile from Mazoria to Chemical Co.	46
4.4	Recommended RGB speed profile from Chemical Co. to Mazoria	46
4.5	Recommended RGB speed profile from Meskel square-1 to Legehar	47
4.6	Recommended RGB speed profile from Legehar to Meskel square-1	48
4.7	Constant braking rate speed profile from Meskel square-1 to Legehar	48
4.8	Constant braking rate speed profile from Legehar to Meskel square-1	49
A.1	Constant braking rate speed profile from Ayat-2 to Ayat-1	56
A.2	Constant braking rate speed profile from Ayat-1 to Ayat-2	57
A.3	Constant braking rate speed profile from Mazoria to Chemical Co.	57
A.4	Constant braking rate speed profile from Chemical Co. to Mazoria	58

List of Tables

1.1	Configuration of artificial bee colony algorithm	4
3.1	AALRT vehicle parameters for adhesion force calculation[5]	37
3.2	Inter-station gradient resistance of AALRT vehicle [5]	39
3.3	AALRT vehicle parameters used for running resistance calculation[5, 6] .	39
3.4	AALRT vehicle parameter for tractive force calculation[5, 6]	40
4.1	Maximized RGBE between Ayat-2 and Ayat-1 station	44
4.2	Maximized RGBE between Mazoria & Chemical Co. station	45
4.3	Maximized RGBE between Meskel square-1 & Legehar	47
4.4	Regenerated energy using constant braking rate b/n Meskel square-1 & Legehar	47
A.1	The AALRT rail gradient profile from Ayat-2 to Tor-hayloch [5]	58

Nomenclature

List of Abbreviations

S-2	Square 2
AALRT	Addis Ababa Light Rail Transit
ABC	Artificial Bee Colony
AREA	American Railway Engineering Association
BG	Broad Gauge
CBR	Constant braking rate
EA	Evolutionary Algorithm
GA	Genetic Algorithm
GP	Evolutionary Algorithm
GP	Genetic Programing
IABC	IArtificial Bee Colony
kg	Kilogram
MG	Metre Gauge
MJ	Mega Joule
NG	Narrow Gauge
N	Newton

RGBE	Regenerative Braking Energy
RGB	Regenerative Braking
S-1	Square 1
SG	Standard Gauge
Co.	Corporation
KE	Kinetic Energy
RGBP	Regenerative braking Power

List of Symbols

$\phi_{i,j}$	Uniform random number
C_x^B	Bogie drag coefficient
ch_k	Choatic variable
α	Angle of inclination or elevation of rail
η	Energy transfer efficiency
η_{re}	Regenerative braking efficiency
η_{rg}	Mechanical to electrical energy conversion efficiency
λ	Creep rate or slip
μ_a	Adhesion coefficient
μ_{max}	Maximum instantaneous adhesion coefficient
ω	Angular velocity of wheel
$\psi_{i,j}$	Uniform random number b/n [0,C]
ρ	Density of air
A	Davis coefficient "A"

NOMENCLATURE

a_1	constant
a_2	constant
A_c	Crossection area
$a_{br_k}^a$	Average braking deceleration
$abs(.)$	absolute value of .
B	Davis coefficient "B"
B_1	Davis coefficient " B_1 "
b_1	constant
B_2	Davis coefficient of air drag momentum " B_2 "
b_2	constant
C	Davis coefficient "C"
c_2	constant
C_d	Drag coefficient
C_x	Head tail drag coefficient
D	Degree of curve
d	Perimeter of train
E_{eb}	Effective electrical braking energy
E_{rg}	The regenerated electrical power
E_{tb}	Total braking energy
$F(x)$	Cost function of ABC algorithm
F_a	Adhesive force
F_b	Braking force

NOMENCLATURE

F_f	Frictional force
F_N	Normal force
F_{eb}	Effective electrical braking force
F_{eb}^{max}	Maximum braking effort of train
F_{te}	Tractive effort of engine
F_{te}^{max}	Maximum tractive effort of train
$fit(.)$	Food source fitness
g	Earth graviataional acceleration
I_g	Inter-vehicle gap
j	Jerk of vehicle
K	Constant which depends on train design
k_m	Rotational mass coefficient
L	Length of train
M	Total mass of train
M_{ef}	Effective mass of train including rotary effect
M_{pc}	Total mass of power car
M_{tc}	Total mass of trailer car
n	Number of axles
N_B	Number of bogies
N_E	Number of employed bees
N_p	Number of pantographs
N_{pc}	Number of power cars

NOMENCLATURE

N_{tc}	Number of trailer cars
P_{max}	Maximum power delivered by engine
P_{rg}	The regenerative braking power
r	Radius of curvature
R_b	Basic or running resistance force
R_c	Curve resistance force
R_g	Grade or gradient resistance
r_w	Radius of the wheel
S	Cross-sectional area
s	Distance or relative location
SN	Number of food source
t	Time
v	Instantaneous translational speed of train
v_a	Relative speed of train with respect to air
v_g	Relative speed of train with respect to ground
v_w	Head wind speed
W	Weight of railway vehicle
$x_{best,j}$	Best solution of current iteration
$x_{i,j}$	Instant food source
x_j^{lb}	Lower limit of food source
x_j^{ub}	Upper limit of food source

Contents

Acknowledgement	i
Abstract	ii
List of Figures	iii
List of Tables	iv
Nomenclature	v
1 Introduction and Background	1
1.1 Background	1
1.2 Problem Statement	3
1.3 Objectives of Research	3
1.3.1 General objective	3
1.3.2 Specific objectives	3
1.4 Methodology	3
1.5 Contribution of The Thesis	4
1.6 Thesis Organization	5
2 Theoretical Background and Literature Review	6
2.1 Dynamics of Railway Vehicle	6
2.1.1 Basic resistance	7
2.1.2 Estimation of Davis coefficient	9
2.1.3 Variant of Davis equation in different country	10
2.1.4 Standard rail gauge	12
2.1.5 Curve resistance	13
2.1.6 Gradient and grade resistance	16
2.1.7 Adhesive force	17
2.1.8 Tractive effort of train	20

2.1.9	Regenerative braking force	21
2.2	Discrete Time Model of Railway Vehicle	21
2.2.1	Braking distance, time, and acceleration	21
2.2.2	Jerk	24
2.2.3	Regenerative braking force, efficiency and energy	25
2.3	Artificial Bee Colony Algorithm	27
2.3.1	Original artificial bee colony algorithm	28
2.3.2	Drawback of original ABC algorithm	31
2.3.3	Variants of artificial bee Colony algorithm	31
2.4	Literature Review of Related Articles	34
2.4.1	Related research v in regenerative braking	34
2.4.2	Related research in ABC algorithms	36
3	Case Study	37
3.1	Adhesion Force of AALRT System	37
3.2	Grade Resistance of AALRT Vehicle	38
3.3	Running Resistance of AALRT Vehicle	38
3.4	Available Tractive Effort of AALRT Vehicle	39
3.5	Electrical Braking Force of AALRT Vehicle	40
4	Results and Discussion	43
4.1	The Total Regenerable Electrical Energy	43
5	Conclusion	50
5.1	Limitation of The Research	50
6	Bibliography	51
Appendices		
A		56
A.1	Extra simulation result	56
A.2	Addis Ababa LRT gradient profile	58

Chapter 1

Introduction and Background

1.1 Background

The electrified railway transportation service is one of public transport system which is used to address mass passenger traffic in urban area. This transportation system is characterized by short distance between stations. It has high capacity, reliability, safety, and environmental friendliness [7]. Therefore, it become effective and sustainable solution for handling mass passenger traffic [7].

Traditional railways uses diesel engine that generate energy within the train, but modern electrified railway transportation systems are energized by electric power which is generated long distance away from the train. Therefore, the system requires transmission line to utilize it. Most railway transportation systems use 600V, 750V, 1500V, 3000V DC power distribution network [7]. The supplied electric power is consumed by the train propulsion, and services like air-conditioning, lighting etc [8]. Among these, the 60 – 70% of total energy consumption is used for generating propulsion [9]. Therefore, reduction of traction energy consumption can minimize the operational cost of transportation system. And this plays significant role in making railway transport service competitive and sustainable even if energy cost is constantly rising [7, 8]. The energy loss of electrified railway transportation system is also depends on transmission line voltage level and instant load. A previous research on metro system shows that the resistive loss increase with decrease in line voltage. Particularly, it is about 22% in 600V, 18% in 750V, 10% in 1500V and 6% in 3000V DC distribution network [7].

Minimizing energy consumption of railway transport system can be achieved either by reducing energy consumption or increasing regenerated energy [8]. The railway vehicle traction energy minimization techniques can be categorized into operational strategies and energy efficient system design. Unlike regenerative braking, these techniques min-

imize power consumption on-line rather to compensate consumed energy by restoring it. The operational strategies minimize energy consumption according to vehicle and infrastructure conditions [8]. It includes time table and driving scheme optimization. The time table optimization is achieved by deciding the optimal drive, brake and dwell time of trains on the same network. The railway vehicle consume large electrical energy to overcome all resistive force and accelerate from rest to full speed and need no power while braking to halt. Therefore, time table optimization is intended to match this two operations carefully to reduce transmission line power loss. During this optimization, the consecutive trains on the same rail should be kept in safe distance to avoid any possible collision. Therefore, the complex signaling and automatic emergency braking system is required to warn and keep range gets safe [10].

In regenerative braking operation, the kinetic energy of train is used to generate electric power [4]. It is attained when the motor turns faster than command speed set by driver [11]. Therefore, it restores fraction of consumed electrical energy [8]. Researchers in [7] show that about 33% of traction energy can be restored to electric power by regenerative braking. This converts a decelerating train to instant electric generator. The regenerated energy can be stored in on-board energy storage devices, feed to the other train on the same network, or return back to the AC distribution line [12]. But in DC powered traction system, regenerated electrical energy can be utilized while other train is on the same network. Otherwise, it will be dissipated in rheostat resistor bank using dynamic braking [4, 11]. But the aim of regenerative braking is to generate and use electrical energy while decelerating a train. Thus in light load condition, this energy is usually stored in on-board batteries or in road side capacitor banks to electrify train and other auxiliary systems in non-electrified zones[7, 11]. Besides, the on board energy storage devices increase the capacity of power supply network by fulfilling extra energy demand to support instant loads. This makes distribution network to supply constant power and stay undisturbed due to sudden load disturbance [12].

The Addis Ababa light rail transit vehicle is powered by 750 *volts* DC power distribution network[5, 6]. Such urban transportation service is characterized by short inter station gap [5]. Thus in order to provide safe transportation service, the Addis Ababa railway vehicle has both mechanical and electrical braking system [5, 6]. As compared to mechanical brake, the electrical brake can restore consumed electric power and reduce physical wear out of brake disk, but it cannot stop a train to halt [4]. As the result, electrical braking system cannot be used for emergency stop [4]. Therefore, in order to take the advantages of electrical braking, it is a common tradition in railway industry to decelerate train using electrical braking and apply mechanical brake at last [4].

1.2 Problem Statement

Now the time energy cost is continuously increasing in this world. At the same time, our country is striving to overcome electric power shortage by constructing hydro-power dams, distributing energy efficient compact florescent lamps, etc. Besides, there is strong competition in developing advanced personal and mass passenger transport systems in the world. Even though the Addis Ababa railway vehicle can use regenerative braking, its energy restoration capacity has not exploited very well yet. Therefore, it is important to exploit electrical energy regeneration capacity of the railway vehicle to reduce its energy consumption and to make it a competitive, energy efficient public transport service of the city.

1.3 Objectives of Research

1.3.1 General objective

The main objective of the research is to enhance regenerative braking energy in railway vehicle of Addis Ababa by using Improved Artificial Bee Colony algorithm.

1.3.2 Specific objectives

The specific objectives of the research are:

1. to study the mathematical model of railway vehicle in Addis Ababa.
2. to enhance regenerative braking energy by developing a braking speed profile which maximize it.
3. to investigate implementation of IABC algorithm for maximizing regenerative braking energy.

1.4 Methodology

The research problem is solved by using the Artificial Bee Colony algorithm which is designed for unconstrained problem. The artificial bee colony algorithm is developed based on the open source available on [13] and [14]. The source code of ABC algorithm is modified for realization of research in [15]. The artificial bee colony algorithm parameters and model of system are configured for the following parameters:

Table 1.1: Configuration of artificial bee colony algorithm

Population size	Onlookers bees	Employed bees	Scout bees	Maximum iteration	Abandonment limit
50	25	25	1	100	15

- The trial limit of food source or abandonment criteria is calculated using equation 1.1 [14].

$$Trial\ limit = 0.6 \times number\ of\ parameter \times number\ of\ source \quad (1.1)$$

- The maximum iteration of algorithm is set to product of total population and size of searched variable [16].

$$I_{max} = Population\ size \times parameter\ size \times 2 \quad (1.2)$$

- The exploitation is done by onlooker bees which select food source based on probability of its improvement. In this thesis, the onlooker bees are forced to make their choice among available sources as shown in equation 2.102.
- The maximum iteration of chaotic search is set to one while it update the best solution of algorithm.
- The railway vehicle deceleration in each discrete searching interval (states) is assumed to be constant, but not necessarily equal to maximum deceleration.
- The rotary mass coefficient of train is assumed as unity, and curve resistance is neglected [17].
- In general, the maximization of regenerative braking is achieved by searching for traveled distance in fixed interval of speed change.
- Each speed profile determined after running the algorithm five times to see the reproducibility of result in *MATLAB-2015*.

1.5 Contribution of The Thesis

This research contributes:

1. the braking speed profile for maximum electrical energy restoration in railway vehicle of Addis Ababa using IABC algorithm.

2. the modification to probability based selection criteria of onlooker bees to increase its exploitation performance.

1.6 Thesis Organization

This thesis is organized into five chapters. The first chapter of the thesis discusses background of the study, statement of problem followed by methodology, objective, limitations and contribution of the study.

In chapter two, theoretical background and literature reviews of articles used in developing the mathematical model of the AALRT system is discussed. Besides, the trend of exemplary countries railway industry in updating Davis equation and adhesion coefficient is reflected. Since the research uses ABC algorithm for optimization, the discretized space model of equivalent analytical formulas are discussed in the aforementioned chapter. Furthermore, variants of artificial bee colony algorithm, modifications done by other researchers to improve its exploitation performance are discussed in detail. In literature review section of chapter two, comparison of this thesis and the most related recent research works is discussed. In addition, the modification done in IABC algorithm probability based selection criteria is reflected with the mathematical verification.

The chapter three of the research discusses a mathematical model of AALRT vehicle and corresponding assumptions. In this chapter, the characteristic of AALRT system is presented both graphically and tabularly based on its convenience.

The result and discussion of the research is compiled in chapter four. The simulation results are presented both graphically and tabularly for selected train stations. The last chapter of this thesis mentions conclusion and limitation of the research.

Chapter 2

Theoretical Background and Literature Review

In this chapter, essential theoretical background required to develop the mathematical model of AALRT system will be discussed. The chapter also covers topics focusing on the trends in updating Devis equation and adhesion coefficient. Furthermore, it includes detail concepts of Artificial bee colony algorithms for global optimization. The final section of the chapter discusses literature reviews of most recent and related researches.

2.1 Dynamics of Railway Vehicle

In most railway system energy optimization researches, a point-mass model of locomotive is used to represent dynamic characteristic of a train. The differential equation representation of train, which is known as Lomonosoff's equation, is used to generate the train states [4, 18].

$$M_{ef}\dot{v}(t) = F_{te}(v) - F_b(t) - R_b(v) - R_g(s) \quad (2.1)$$

Where, M_{ef} is the effective mass of train including rotary effect;

F_{te} is the tractive effort of engine;

F_b is the applied braking force;

R_b is the running or basic resistance of train;

R_g is gradient resistance;

s is distance or relative location;

t is the instantaneous time;

v is the instantaneous speed.

In addition to gradient and running resistance, there is resistive force that oppose motion of train due to the curve rail. This force is known as curve resistance (R_c) [19]. Including the curve resistance in point-mass model of train, equation 2.2 is obtained.

$$M_{ef}\dot{v}(t) = F_{te}(v) - F_b(t) - R_b(v) - R_g(s) - R_c(r(s), v) \quad (2.2)$$

In regenerative braking operation, the tractive effort of train is set to zero. Therefore, equation 2.2 is rewritten as follows [4].

$$M_{ef}\dot{v}(t) = -F_b(t) - R_b(v) - R_g(s) - R_c(r(s), v) \quad (2.3)$$

2.1.1 Basic resistance

The basic resistance of train is the total resistive force against its motion on level track in still air at constant speed. It includes the rolling resistance, bearing resistance, the frictional force between the rail and flange, and aerodynamic resistance of train [20]. Generally, the running resistance is described by quadratic function which is formulated by run down tests [18, 19]. This quadratic equation is known as the "von Borries Formel", the "Leitzmann Formel", the "fonction de Barbier" and, in Anglo-Saxon world, the Davis equation [19].

$$R_b = A + Bv + Cv^2 \quad (2.4)$$

Where, v is the instantaneous speed of train and A, B and C are Davis coefficient.

The equation 2.4 shows the train resistance in open and still air. In condition where ambient wind exist, not only the term B but also aerodynamic coefficient C is affected [21].

$$R_b = A + B_1v_g + B_2v_a + Cv_a^2 \quad (2.5)$$

Where: v_g is the train speed relative to ground

v_a is the train speed relative to the air

The Davis coefficient "A" is predominantly mechanical resistance. It linearly increase with number axle and slightly with load per axle. Besides, it depends on mass of railway vehicle, brake and transmission drag, track design, wheel diameter, etc [17, 19, 21]. Further more, this resistance can be resolved into journal friction and rolling friction. The former depends on type of lubrication, bearing, temperature and condition, internal resistance which is caused by movement of its mechanical body parts. The rolling resistance refers to the frictional force between wheel and rail [2]. For train of mass M , the range of Davis coefficient (A) is given by equation 2.6 [21].

$$\frac{A}{M} = 0.005 \text{ to } 0.02 N/kg \quad (2.6)$$

The Davis Coefficient "B₁" represent the friction due to viscous component of mass including impact between the wheel flanges and rail due to sway, concussion, buff and slack-action. It is estimated to be in range of $1.0 \text{ to } 2.0 \times 10^{-4} v \text{ N/kg}$, where v is instantaneous speed of train [20, 21].

The Davis coefficient "B₂" is referred to air momentum drag. It refers to the energy required to ingest air for combustion of diesel engine and air conditioning. In modern train it range from $0.2 \text{ to } 0.5 v \text{ N/length train in meter}$, where v is speed [20, 21].

The Davis coefficient "C" is refers to the aerodynamic characteristic of train which is described by equation 2.7 for still open-air [21].

$$Cv_a^2 = \frac{1}{2} C_d \rho v_a^2 A_c \quad (2.7)$$

Where: C_d is drag coefficient;

ρ is the density of air;

A_c crossection area of train;

v_a speed of train relative to air.

The first two terms of Davis equation i.e. A and B are dominant at low speed less than 30 m/s because they mainly represent resistance due to train mass. The term Cv^2 , which stand for the aerodynamic friction between surface of train and drag force, is dominant at higher speed. Usually, the Davis equation is stated for open air thus, it require modification for tunnel operation where aerodynamic resistance is much more greater than that of open air [17, 19, 20]. The factors that affect the aerodynamic resistance of train can be categorized into two [21]:

1. pressure drag is caused by distribution of static pressure over the external surface of train
2. skin effect is due to the airflow viscosity that produce shear force at the surface of train. In modern passenger train with smooth surface, the skin effect cause a decrease in drag coefficient.

Besides, the combined influence of both pressure drag and skin effect such as boundary layer pressure drag and interference effect varies the drag coefficient.

2.1.2 Estimation of Davis coefficient

Armstrong and Swift equated the formula to estimate value of Davis coefficient for electric multiple unit train in service at the time of former British Rail [17, 19].

$$A = 6.4M_{tc} + 8.0M_{pc} \quad (2.8)$$

$$B = 0.18M_{train} + 1N_{tc} + 0.005N_{pc}P_{total} \quad (2.9)$$

$$C = 0.6125C_xS + 0.00197dL + 0.0021dI_g(N_{tc} + N_{pc} - 1) + 0.2061C_x^B N_B + 0.2566N_p \quad (2.10)$$

Where: M is the total mass of train car in *tons*;
 M_{tc} is the total mass of trailer car in *tons*;
 M_{pc} is the total mass of power car in *tons*;
 N_{pc} is the number of power cars;
 N_{tc} is the number of trailer cars;
 N_p is the number of pantographs;
 N_B is the number of bogies;
 S is the cross-sectional area in m^2 ;
 d is the perimeter in *meter*;
 L is the length of train in *meter*;
 C_x is the head/tail drag coefficient;
 C_x^B is the bogie drag coefficient;
 I_g is the inter-vehicle gap.

2.1.3 Variant of Davis equation in different country

The Davis formula of running resistance is modified in several country to fit modernization of railway vehicle. The railway industry in France, German, USA, and Japan have determined the value of Davis coefficients based on field test data. Even though the general form of Davis formula is uniform, the difference in railway vehicle specification of those countries leads to significant difference in value of Davis coefficient [19].

France

The French national railway, SNCF, has developed running resistance equation for different train in their country. The empirical formula which is stated by SNCF for the diesel or electric locomotive is given by [19]:

$$R_b = 0.0065L + 0.13n + 0.0036v + 0.003888v^2 \quad (2.11)$$

Where: L is the locomotive mass in tone;

n is the number of axle;

v is the speed in m/s .

For electric multiple units with traction motor on several vehicles the running resistance is given by equation 2.12.

$$R_b = (0.013\sqrt{\frac{10}{m}} + 0.00036v)P + 0.1296Cv^2 \quad (2.12)$$

$$where \quad C = 0.0035s + 0.0041\frac{pL}{100} + 0.002N \quad (2.13)$$

Where: P is the total EMU mass in tone;

m is the mass per axle in tone;

v is the speed in m/s ;

S is the front cross sectional area of train m^2 ;

p is the partial perimeter of rolling stock down to rail in meter, usually $10m$;

L is the train length in meter;

k_1 is the constant that varies with front and rear shape $\in [9 \times 10^{-4}, 20 \times 10^{-4}]$;

k_2 is the parameter that depends on surface condtion;

N is the number of raised pantograph.

German

In German railway industry, the Strahl formula is used for the freight and mixed passenger train, and Sauthoff formula is used for intercity passenger train [19].

$$R_b = 0.01((1.5 - 2.5) + (0.007 + \frac{1}{m})(\frac{3.6v}{10})^2) \quad (2.14)$$

Where: R_b = 10 running resistance in N/kg ;

v = 10 train speed in m/s ;

$$m = \begin{cases} 40 & \text{for four-axle passenger coaches and freight wagon;} \\ 30 & \text{for two and three-axle passenger carriages;} \\ 25 & \text{for loaded wagons in express parcel trains;} \\ 10 & \text{for empty freight wagons.} \end{cases}$$

Sauthoff formula describes basic resistance (R_b) of train with n coach and Q mass.

$$R_b = [1.9 + 3.66bv + 0.0048\frac{1}{Q}(n + 2.7)A(3.6v + v_w)^2] \quad (2.15)$$

Where $R_b = 1.45m^2$ is the basic resistance in N/kg ;

$v_w = 15km/h$ is head wind speed.

$$A = \begin{cases} 1.45m^2 & \text{equivalent area for fast train on new high speed lines;} \\ 1.55m^2 & \text{for fast train on other line;} \\ 1.15m^2 & \text{for two and three-axle passenger carriages.} \end{cases}$$

$$b = \begin{cases} 0.0025 & \text{for four axle vehicle;} \\ 0.004 & \text{for three axle vehicle;} \\ 0.007 & \text{for two axle vehicle;} \end{cases}$$

USA

The American Railway Engineering Association has updated the Davis formula for modern railway technology. The modified Davis equation consider the rolling, journal, track, flange and aerodynamic resistance. This Davis equation is used for determination of modern light railway vehicle basic resistance in Chicago and Portland [22].

$$R_B(v) = \left(0.6 + \frac{20}{w_p} + \frac{0.01v(t)}{1.61} + \frac{C_d(v(t)/1.61)^2}{w_p n_p}\right) \times M \times 4.4482 \quad (2.16)$$

Where w_p is weight per axle of vehicle including passenger mass, n_p is number of axles, C_d is head-tail aerodynamic drag coefficient of vehicle (usually $C_d = 0.07$). The variable "K", which is used by [22] to represent aerodynamic drag coefficient, is changed to " C_d ". The speed of $v(t)$ is given in kph, mass M in *ton* and 4.4482 is used to convert *lb* to *N* by author [22].

2.1.4 Standard rail gauge

The gauge of railway track is a description of perpendicular distance between the inner face of the two rail. The size of rail gauge is affected by traffic condition, budget, desired speed of train and nature of country. Based on magnitude of the perpendicular distance

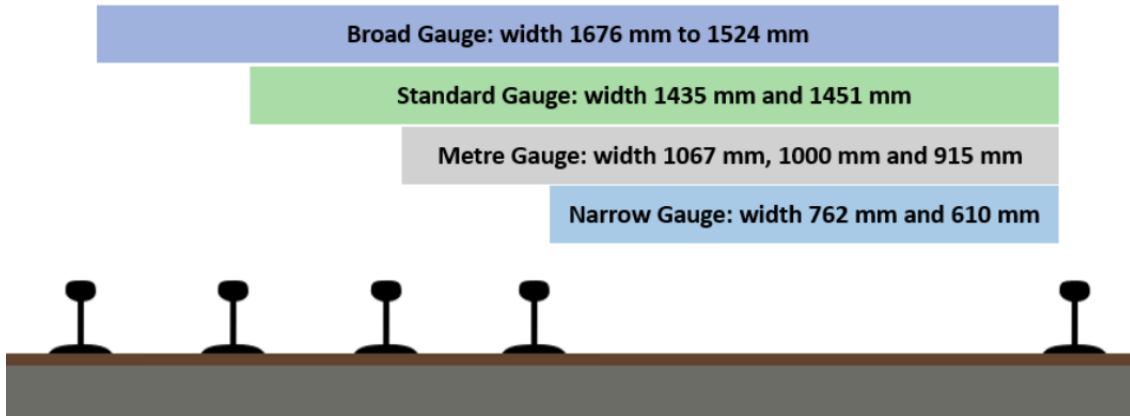


Figure 2.1: Rail gauge types [1]

between rail, the gauge of railway track is categorized into four types [1]. Namely :

1. Broad Gauge (BG) : breadth range from 1524 *mm* to 1676 *mm*
2. Standard Gauge (SG) : breadth range from 1435 *mm* to 1451 *mm*
3. Metre Gauge (MG) : breadth range from 1000 *mm* to 1067 *mm*
4. Narrow Gauge (NG) : breadth range from 610 *mm* to 762 *mm*

2.1.5 Curve resistance

The curve resistance is the additional opposition force that should be overcome by tractive effort of train as it passes through a horizontal curve track. The main causes of curve resistances are [2, 23]:

1. the rigid base of wheel that causes poor adaptation of railway vehicle to curved track. For this reason, friction is developed between flange of the leading axle outer wheel and the inner face of outer rail, and inner wheel of trailer axle of the bogie and inner face of the inner rail as shown in Figure 2.2.
2. the transverse slip which is caused by faster speed of outer wheel relative to inner wheel of bogie causes additional sliding friction.
3. longitudinal slip, that causes the sliding motion of wheel while outer wheel flange of trailer axle remains clear and tends to derail.
4. poor super elevation of rail which increases the pressure on outer rail while excess super elevation exerts more pressure on the inner rail. As a result, curve resistance increases.
5. poor maintenance is the main cause of bad alignment, worn out rail and improper level that increases the curve resistance.

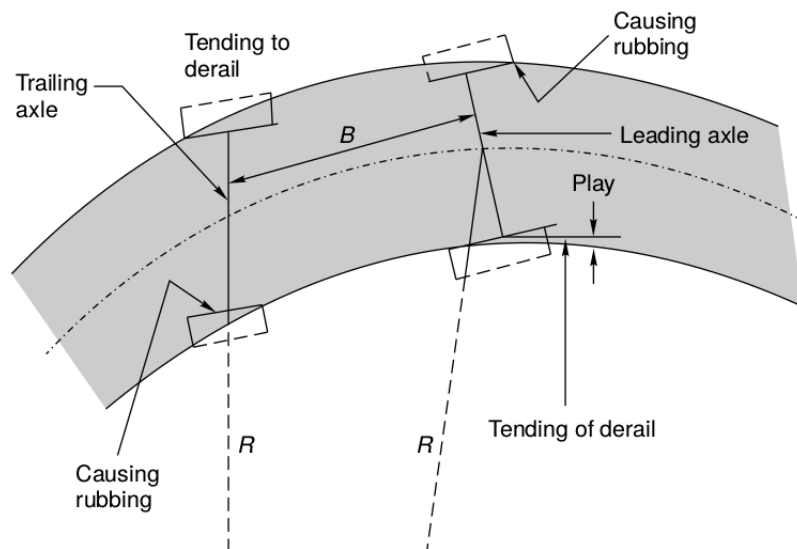


Figure 2.2: Curve resistance [2]

The super elevation of rail, which is a banked railroad on the curve, is used to minimize centrifugal force on the curve. For this reason, there might even be negligible curve resistance

at lower speed of train. Besides, it has small effect for large radius curve of track. Therefore, the curve resistance is usually ignored except for tight curves whose radius is less than $250m$ [19].

The curve resistance of railway vehicle varies not only with radius of curvature, but also with type of rail gauge and magnitude of sliding friction between wheel flange and rail. It is directly proportional to the rail gauge and sliding friction, and inversely proportional to radius of curvature [2].

$$R_c = C \frac{FG}{R} \quad (2.17)$$

Where: C is the constant;

F is the force of sliding friction;

G is the track gauge;

R is the radius of curve.

There are several empirical formula for calculating curve resistance railway vehicles such as: Roeckl's formula, Profilidis equation etc.

The Roeckl's formula of curve resistance for various type of gauge [3, 18, 24]:

- For standard gauge 1435 mm

$$R_c(r(s)) = \begin{cases} \frac{6.3}{r(s) - 55} M & \text{for } r(s) > 300m \\ \frac{5.19}{r(s) - 35} M & \text{for } r(s) \approx 300m \\ \frac{4.91}{r(s) - 30} M & \text{for } r(s) \leq 250m \end{cases} \quad (2.18)$$

- For meter gauge 1000 m

$$R_c(r(s)) = \frac{3.92}{r(s) - 20} M \quad (2.19)$$

- For gauge 900 mm

$$R_c(r(s)) = \frac{3.726}{r(s) - 17} M \quad (2.20)$$

- For narrow gauge 750 mm

$$R_c(r(s)) = \frac{3.432}{r(s) - 10} M \quad (2.21)$$

- For narrow gauge 600 *mm*

$$R_c(r(s)) = \frac{1.961}{r(s) - 5} M \quad (2.22)$$

Where: R_c is curve resistance in Newton
 $r(.)$ is the radius of curve in meter;
 s is a distance in meter;
 M is mass of train in kilogram.

Profillidis equation of curve resistance, which is commonly used in railway industry, is given by equation 2.23 [17, 19].

$$R_c = 0.01 \left(\frac{K}{r_c} \right) \quad (2.23)$$

Where:

R_c = curve resistance in kN/t assuming earth gravity is $10m/s^2$;
 r_c = radius of curve in meter;
 K = constant that depends on train design and range from 500 to 1200.

The curve resistance of train can also be described as the function of train weight and degree of curve for different type of rail gauges [2, 17, 20].

$$R_c = \begin{cases} 0.0004WD & \text{for Broad Gauge (BG)} \\ 0.0003WD & \text{for Meter Gauge (MG)} \\ 0.0002WD & \text{for Narrow Gauge (NG)} \end{cases} \quad (2.24)$$

Where W is the weight of train and D is the degree of curve.

Normally, curve resistance as 0.04% of upgrade per degree of curvature for standard gauge track and 0.05% upgrade per degree of curve for speed less than 5 *kph* is commonly accepted in railway industries [17, 20].

2.1.6 Gradient and grade resistance

Gradient is a description of the rise and fall in the altitude of railway track. It can be either rising or falling in the direction of motion. Gradient is designed to follow geographic contour, to reduce earth work, and to reach stations at different elevation [2].

Grade resistance occurs due to the altitude profile difference between two consecutive point in railway. This change create inclined surface that decompose the total weight of train into two components.

- Normal force is reactive force of inclined surface in a direction perpendicular to a plane.
- Grade resistance is a tangential component of train weight on inclined surface. Based on direction of train motion, it either parallel or opposite to tractive effort of train [24]. In case of regenerative braking, where braking force is applied by engine, it is parallel to braking force for uphill, and opposite for downhill traction.

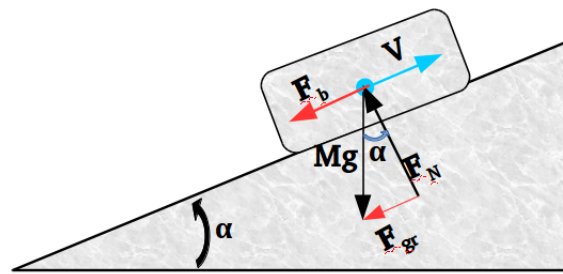


Figure 2.3: Grade or gradient resistance of train

Resolution of weight for point-mass model of railway vehicle on inclined plane as shown in Figure 2.3 is described by [4]:

$$F_N = Mg \cos(\alpha) \quad (2.25)$$

$$R_g = Mg \sin(\alpha) \quad (2.26)$$

Where, F_N – is the normal force

M – is the tare mass of train

g – is the graviational acceleration

α – is the angle of inclination

2.1.7 Adhesive force

The adhesive force is a tangential force which is transmitted in longitudinal direction between rail and wheel. It is reactive force of rail for action exerted by wheel known as tractive effort. The adhesion arise from inter-atomic interaction between rail and wheel. Since the wheel-rail contact is open system, it can be affected by contaminant such as moistures, lubricants, oxidation, leaves. The ratio of Adhesive force (F_a) to normal force (F_N) is know as adhesion coefficient (μ_a) [25].

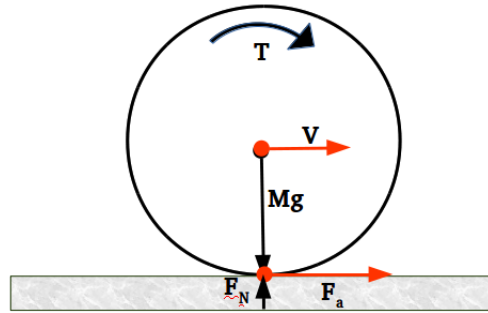


Figure 2.4: Wheel-rail adhesion

$$\mu_a = \frac{F_a}{F_N} \quad (2.27)$$

Adhesive force is different from the friction force that opposes the motion of train. The force required to initiate the motion of object at rest is called static friction while force required to maintain moving object at uniform speed is kinetic friction. The ratio of frictional force (F_f) to normal force (F_N) is known as friction constant (μ_f). For most metallic pairs, range of friction coefficient is 0.00 to 1.00 while range of adhesion coefficient is 0.00 to 0.40. This shows that friction coefficient is greater than that of adhesion both under clean and contaminated condition [25, 26].

$$\mu_f = \frac{F_f}{F_N} \quad (2.28)$$

Assuming a single vehicle whose load is equally distributed among powered axles and wheels, Yi Zhu, in [25], has equated the simplified model for calculating adhesion coefficient.

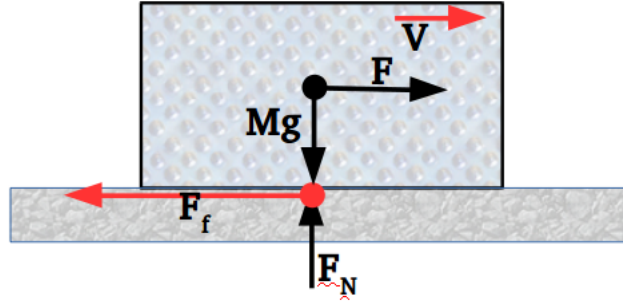


Figure 2.5: Frictional force of sliding block

$$\sum F_N = Mg \quad (2.29)$$

$$F_{ak} = \mu_a F_N \quad (2.30)$$

$$F_a = \sum_k F_{ak} = \mu_a Mg \quad (2.31)$$

The above equation is formulated to calculate the total adhesive force and adhesion coefficient under zero degree angle of inclination. Considering railway vehicle on inclined rail as shown in figure 2.6, the normal force can be calculated by equation 2.32.

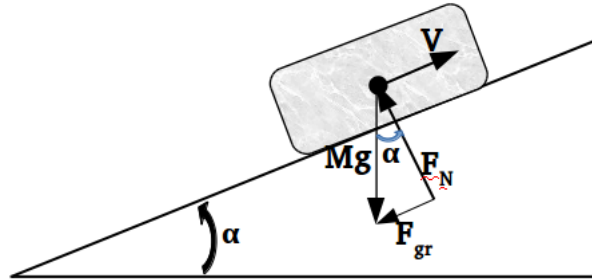


Figure 2.6: Normal force of railway vehicle on inclined surface

$$\sum F_N = Mg \cos(\alpha) \quad (2.32)$$

Therefore, the total adhesive force of a point mass model of railway vehicle is described by equation 2.33.

$$F_a = \mu_a \sum F_N = \mu_a Mg \cos(\alpha) \quad (2.33)$$

Normally, adhesion is described as function of sliding speed which is the difference between translational speed of vehicle and tangential speed of wheel. The adhesion

coefficient varies with speed of train and creep rate or slip. The slip/ creep rate is dimension less quantity which is defined as the ratio of sliding speed to actual translational speed of railway vehicle [27, 28].

$$\lambda = \frac{\omega r_w - v}{v} \quad (2.34)$$

Where: λ is creep rate or slip;
 ω is angular velocity of wheel
 r_w radius of the wheel;
 v is translational speed of train.

Neglecting the effect of speed, the relation of adhesion coefficient and slip or creep rate is described in equation 2.35 [27].

$$\mu(\lambda) = a_1(1 - \exp(-b_1\lambda)) - \frac{\lambda}{10} \quad (2.35)$$

Where a_1, b_1 depends on surface of rail.

The maximum available adhesion coefficient decrease as speed of train increase. If effect of slip is assumed to negligible, the adhesion coefficient as function of speed is given by equation 2.36 [27].

$$\mu_{max}(v) = a_2 + \frac{b_2}{c_2 + v} \quad (2.36)$$

Where a_2, b_2 and c_2 are constants.

Based on equation 2.35 and 2.36, the analytical relation of $\mu(\lambda, v)$ and $\mu_{max}(\lambda)$ is given in equation 2.37 [27].

$$\mu(\lambda, v) = \frac{\mu_{max}(v)}{\mu_{max}(0)}\mu(\lambda) \quad (2.37)$$

Several countries developed different adhesion coefficient model as function of instantaneous speed based on run down test.

The adhesion coefficient for German class 19 railway vehicle with speed range of 0 to 160 *kph* is described by equation 2.38 after field test in 1943 [29].

$$\mu_a = \frac{7.5}{v + 44} + 0.16 \quad (2.38)$$

Where: v is speed of train in kph ;
 μ_a is in percent.

The other equation of adhesion coefficient is formulated by French National Railway (SNCF) by running electric locomotive in 1960s [29].

$$\mu_a = 0.24 \times \frac{8 + 0.1v}{8 + 0.2v}, \quad \text{for } v \text{ in } kph \quad (2.39)$$

Similarly, the field test was done in Japan National Railway (JNR) on Shinkansen 200 locomotive, whose speed range is 0 to 250 kph , for estimating the adhesion coefficient [29].

$$\mu_a = \frac{136}{85 + v}, \quad \text{for } v \text{ in } kph \quad (2.40)$$

2.1.8 Tractive effort of train

The locomotive tractive effort is a driving force of train. It enable the railway vehicle to overcome all resistive force against its' motion and run either in uniform speed or acceleration. The source of railway vehicle tractive effort is either diesel or electric engine. The maximum effective tractive force of train is limited by the adhesive force rail and wheel. In the other word, the driver can increase tractive effort of train up to the maximum adhesive force. As it exceed the adhesion or rolling frictional between rail and wheel, the wheel start skidding rather generating the desired translational motion [4, 30, 31]. The tractive effort of electric locomotive engine as the function of speed is given by equation 2.41 [30, 31].

$$F_{te}^{max}(v) = \frac{\eta \times P_{max}}{v} \quad (2.41)$$

Where P_{max} – maximum power delivered by engine

F_{te}^{max} – maximum tractive effort of train

η – efficiency of energy transfer

v – instantaneous speed of train

The effective tractive effort of railway vehicle is limited by adhesion force between rail and wheel. Its common practice to increase magnitude of tractive effort to attain higher speed in railway industry, but increasing its magnitude beyond the adhesion force of rail will no longer increase translational speed. Instead, the tangential speed of wheel exceed translational speed of railway vehicle. This phenomena is known as slip. This shows that

effective tractive effort of vehicle is not only limited by power of the engine, but also by wheel and rail adhesion force [4, 29].

$$F_{te}(v) = \min(F_a(v), F_{te}^{max}(v)) \quad (2.42)$$

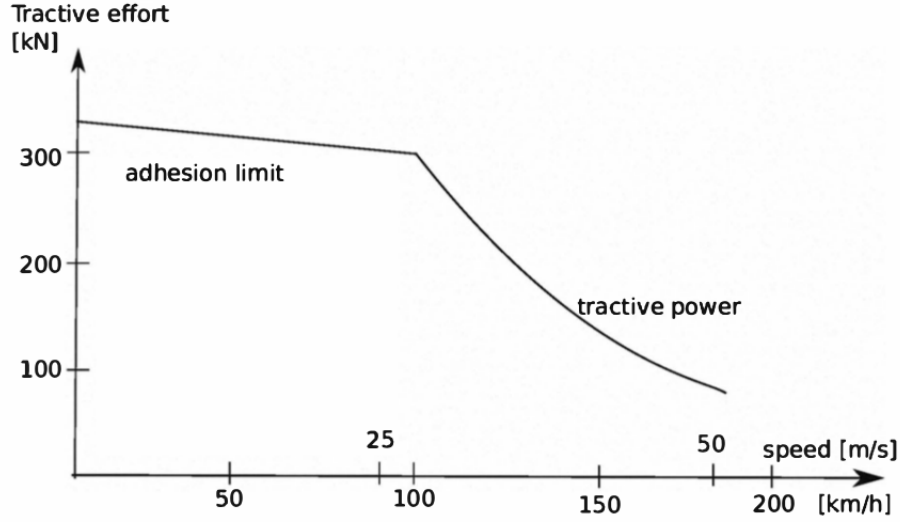


Figure 2.7: Available tractive effort as function of speed [3]

2.1.9 Regenerative braking force

In this research, magnitude of maximum regenerative braking force (F_{eb}^{max}) which can be exerted by the engine is approximated by its maximum tractive effort (F_{te}) at the instant speed $v(t)$ [31, 32].

$$F_{eb}^{max}(v(t)) = -F_{te}(v(t)) \quad (2.43)$$

2.2 Discrete Time Model of Railway Vehicle

2.2.1 Braking distance, time, and acceleration

In regenerative braking system, the braking force is delivered by engine when it act as generator. The it is approximately represented by the maximum tractive force that can be delivered by the engine at instantaneous speed of a train. In each discrete state of searching interval, both gradient and curve resistance are assumed to be constant.

Besides, the uphill traction gradient resistance is considered as positive since it align in the direction of applied braking force [4].

$$M_{ef} \frac{dv}{dt} = -F_b(v) - R_b(v) - R_g(s) - R_c(r(s), v) \quad (2.44)$$

In braking operation, both the initial and final speed of train is known. Therefore, the intermediate speed v_k can be generated from initial speed v_1 to final speed v_N which is zero [4].

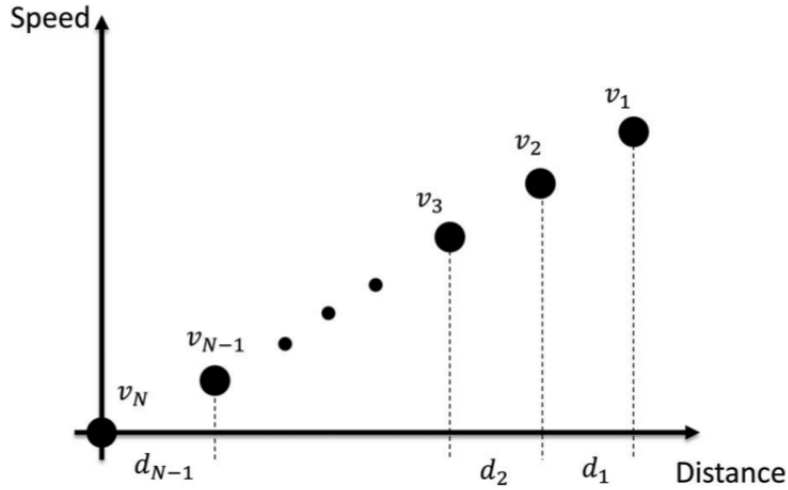


Figure 2.8: Braking speed vs distance for sequential computing [4]

$$v_k = v_1 - (k - 1) \frac{v_1 - v_N}{N - 1} \quad (2.45)$$

Where N maximum number of segment and $k = 2, 3..N$.

The braking acceleration is assumed to be constant or uniform in each discrete state of braking operation [4].

$$a_{br.k} = \frac{v_{k+1} - v_k}{t_{k+1} - t_k} = \frac{v_{k+1} - v_k}{\Delta t_k} \quad (2.46)$$

$$\Delta s_{br.k} = \frac{v_{k+1} + v_k}{2} \times (t_{k+1} - t_k) \quad (2.47)$$

From equation 2.46 and 2.47 the average braking deceleration is described by [4]:

$$a_{br.k} = \frac{v_{k+1}^2 - v_k^2}{2\Delta s_k} \quad (2.48)$$

Where: a_{br_k} – braking acceleration (deceleration)

v_{k+1} – speed of train at time t_{k+1}

v_k – speed of train at time t_k

Δs_k – average travel distance in the interval

The time taken by a train to move the average distance Δs_k as the speed drops from v_k to v_{k+1} can be calculated using equation 2.49.

$$\Delta t_k = \frac{2\Delta s_{br_k}}{v_{k+1} + v_k} = \frac{\Delta s_{br_k}}{v_k^{av}} \quad (2.49)$$

The total braking time become the sum of all Δt_k .

$$T = \sum_{k=1}^{N-1} \Delta t_k \quad (2.50)$$

The average acceleration of a train should be less than the maximum acceleration. This indirectly constrained the minimum distance which must be traveled in each stepping interval.

$$a_{br_k} = \frac{v_{k+1}^2 - v_k^2}{2\Delta s_k} \leq a_{max} \quad (2.51)$$

$$\frac{v_{k+1}^2 - v_k^2}{2a_{max}} \leq \Delta s_k = \Delta s_k^{min1} \quad (2.52)$$

Similarly from equation 2.44 and regenerative energy constraint, the maximum distance that can be traveled by train while regenerative braking operation can be determined [4].

$$E_{ebk} \leq \begin{cases} (M_{ef} \frac{dv}{dt} - R_b(v) - R_g(s) - R_c(r(s), v)) \times \Delta s_k & \text{or} \\ \frac{1}{2} M_{ef} (v_k^2 - v_{k+1}^2) - (R_b(v) + R_g(s) + R_c(r(s), v)) \Delta s_k \end{cases} \quad (2.53)$$

The maximum braking distance is traveled by train when no braking force is applied to it. Thus setting E_{ebk} to zero the following constraint in travel distance is obtained [4].

$$\Delta s_k \leq \Delta s_k^{max1} = abs\left(\frac{0.5 M_{ef} (v_k^2 - v_{k+1}^2)}{R_b(v) + R_g(s) + R_c(r(s), v)}\right) \quad (2.54)$$

2.2.2 Jerk

The acceleration and deceleration are important characteristic of railway vehicle for ad-equate operation of train, but these properties introduce undesired effect known as jerk. The jerk is defined as rate of change in acceleration. In railway industries, not only the magnitude acceleration but also that of jerk is limited for passengers comfort. If those values exceed the limit, passengers might lose their body motion control and get injured [33, 34, 35].

$$j(t) = \frac{da(t)}{dt} \quad (2.55)$$

Numerically it can be approximated by

$$j_k = \frac{a_k - a_{k-1}}{t_k - t_{k-1}} \quad (2.56)$$

Where: j is the jerk;

j_k is the jerk at time t_k ;

a_k, a_{k-1} is the acceleration at time t_k and t_{k-1} respectively;

t_k, t_{k-1} are current and previous time respectively.

Jerk limit

The magnitude of jerk which is defined in equation 2.56 shall never exceed a jerk limit. *(In this calculation, only the magnitude of deceleration is considered.)*

$$j_k = \frac{a_k - a_{k-1}}{\Delta t} \leq J_{max} \quad (2.57)$$

Δt can be determined from average deceleration.

$$\Delta t = \frac{\Delta v}{a_k} \quad (2.58)$$

Then rearranging equation 2.57 the next iteration deceleration can be determined.

$$a_k \leq a_{k-1} + J_{max} \frac{\Delta v}{a_k} \quad (2.59)$$

$$a_k^2 - a_k a_{k-1} - J_{max} \Delta v \leq 0 \quad (2.60)$$

After solving this inequality, the maximum and minimum deceleration, and corresponding upper and lower limit of travel distance which satisfy the constraint in jerk is determined.

$$\frac{a_{k-1} - \sqrt{a_{k-1}^2 + 4J_{max}\Delta v}}{2} \leq a_k \leq \frac{a_{k-1} + \sqrt{a_{k-1}^2 + 4J_{max}\Delta v}}{2} \quad (2.61)$$

$$a_k^{min} \leq a_k \leq a_k^{max} \quad (2.62)$$

The minimum limit in a_k leads to upper bound of distance while maximum limit in equation 2.62 leads to lower bound.

$$\Delta s_{min2} = \frac{v_{k+1}^2 - v_k^2}{2min(a_k^{max}, a_{max})} \quad (2.63)$$

$$\Delta s_{max2} = \frac{v_{k+1}^2 - v_k^2}{2min(a_k^{min}, a_{max})} \quad (2.64)$$

Finally, the upper bound of search operation is Δs_k^{max} and the lower bound of the distance Δs_k^{min} which should be traveled by vehicle to satisfy the maximum deceleration and jerk is determined. Therefore, a possible solution Δs_k which satisfies the required criteria of safe and comfortable braking operation with maximum energy restoration is searched between upper and lower bound of distance.

$$\text{Where: } \max(\Delta s_k^{min1}, \Delta s_k^{min2}) \leq \Delta s_k \leq \min(\Delta s_k^{max1}, \Delta s_k^{max2}) \quad (2.65)$$

Finally, the total braking distance becomes the sum of all Δs_k [4].

$$D = \sum_{k=1}^{N-1} \Delta s_k \quad (2.66)$$

2.2.3 Regenerative braking force, efficiency and energy

The regenerate braking effort is approximated by the tractive force of locomotive which is delivered at instantaneous speed of railway vehicle. If F_{eb}^{max} is the maximum available regenerative braking force at the instantaneous speed $v(t_k)$, applied electrical braking force F_{eb} should not exceed the total braking force which is given by equation 2.68 [4].

$$F_{eb}^*(v_k) = \min(F_{tb}(v_k), F_{eb}^{max}(v_k)) \quad (2.67)$$

$$F_{tb} = M_{ef} a_{br_k} \quad (2.68)$$

Where: F_{eb}^* is the applied electrical braking force;

F_{tb} is the total braking force;

a_{br_k} is the braking deceleration;

M_{ef} is the effective mass of vehicle including rotary effect.

The effective mass of railway vehicle is a product of its total mass and coefficient of rotational mass (k_m) [4, 36].

$$M_{ef} = k_m \times M_t \quad (2.69)$$

In railway industry, the retarding acceleration is limited or bounded to maximum braking deceleration (a_{br}^{max}) for safety and passenger comfort under normal braking operation. This constraint indirectly limits the maximum braking force (F_{br}^{max}) which should be exerted on railway vehicle. For this reason, applied effective regenerative braking force must fulfill this restriction [3].

$$F_{eb}(v_k) = \min(F_{eb}^*(v_k), F_{br}^{max}) \quad (2.70)$$

$$F_{br}^{max} = M_{ef} a_{br}^{max} \quad (2.71)$$

The total braking energy ($E_{tb}(v_k)$) is the work done in each interval of braking operation by the braking force as vehicle travel distance (Δs) with average speed (v_k^a) [4, 36].

$$E_{tb}(v_k) = F_{tb}(v_k^a) \Delta s \quad \text{where } v_k^a = \frac{v_{k+1} + v_k}{2} \quad (2.72)$$

It can be described as product of railway vehicle mass, average deceleration (a_{br}) and traveled distance (Δs) or change in kinetic energy. [4, 36]

$$E_{tb} = M_{ef} a_{br.k} \Delta s = \frac{1}{2} M_{ef} (v_{k+1}^2 - v_k^2) \quad (2.73)$$

The electrical braking energy can be described as the work done by effective electrical braking force. It can be calculated from equation 2.3 as [4]

$$F_{eb}(t_k) = F_{tb}(t_k) - R_b(v_k^a) - R_g(s_k) - R_c(r(s_k), v_k^a) \quad (2.74)$$

$$E_{eb}(v_k^a) = F_{eb}(v_k^a) \Delta s \quad (2.75)$$

There is energy loss in engine power transmission system, in motor when it act as generator and in power electronics devices. For this reasons, not all available kinetic energy of the vehicle is converted to electrical and returned back to the power supply system. Therefore, the regenerated power in terms of total power of vehicle is described in equation 2.77 [36].

$$P_{rg} = \eta_{rg} k_m M_t a_{br_k} v_k^a \quad (2.76)$$

$$= \eta_{rg} M_{ef} a_{br_k} v_k^a \quad (2.77)$$

Where: P_{rg} is the regenerative braking power;
 k_m is the coefficient of rotational mass;
 M_t is the total mass of railway vehicle;
 M_{ef} is effective mass of railway vehicle;
 $a_{br_k}^a$ is the average braking deceleration;
 v_k^a is the average instantaneous speed of train;
 η_{rg} is the efficiency of mechanical to electrical energy conversion.

Considering electric power loss, the regenerated energy (E_{rg}) is described in equation 2.78 in terms of the total available electrical braking energy (E_{eb}) and regenerative efficiency (η_{re}) [4, 22].

$$E_{rg} = \eta_{re} E_{eb} = \eta_{re} F_{eb} \Delta s \quad (2.78)$$

Where: η_{re} = regenerative braking efficiency.
 F_{eb} = instantaneous effective electrical braking force.

The regenerative efficiency describes the part of total braking energy that can be successfully restored. The regenerative efficiency (η_{re}) is modeled as exponential function by J. Wang and Rakha. This modeling of regenerative efficiency represent the actual restored power with uncertainty of 1.87% to -2.31% while constant efficiency model cause 10.77% to 16.11%. Thus in this thesis, the regeneration efficiency modeling recommended by J. Wang and Rakha is used. The value of regenerative efficiency model parameter (α_{re}) is equals to (0.65) [22].

$$\eta_{re}(t) = \begin{cases} \exp(\frac{-\alpha_e}{|a_{br}(t)|}) & \text{for } a_{br} < 0 \\ 0 & \text{otherwise} \end{cases} \quad (2.79)$$

2.3 Artificial Bee Colony Algorithm

The population based algorithms is one of heuristic algorithm which is used in numerical optimization problems. In the population based algorithms, each members consists of

possible solution and corresponding fitness for the optimization problems. Based on the fitness value of the solution, it may pass through several modification to generate new better solution. Based on the natural phenomena simulated by the algorithm, population based algorithms are categorized into evolutionary based and swarm intelligent based algorithm. The evolutionary algorithm consists of Genetic Algorithm (GA), Genetic Programing (GP), Evolutionary Algorithm (EA) and Evolutionary Programing(EP). The swarm intelligence algorithms imitate the forging properties of social insects, such as bees, ants, termites and wasps, behaviors for solving numerical optimization problem. The collection of any interacting agents such as ants, bees, flocks of birds and human immunity cells are considered as swarm. Based on the nature of aforementioned swarms, several optimization algorithms have been developed by researchers. For instance: Ant colony algorithm from ants, Artificial bee colony algorithm from bees, Particle swarm optimization algorithm from birds flocks or fish schools and Artificial immune system algorithm from immune cells of human beings [37, 38, 39].

2.3.1 Original artificial bee colony algorithm

The artificial bee colony algorithm is one of swarm intelligent based algorithm that models foraging behavior of honey bees. In developing the swarm intelligence algorithm, identifying the self-organization and labor division behavior of swarm is a key to simulate them for solving any optimization problems. The minimal model of honey bees consists of food sources, employed and unemployed foragers [38].

1. Food source: The value of food source represents its distance from the nest, amount of nectar and complexity of extraction [38].
2. Employed foragers: They consists a group of bees which are currently exploiting the source and carry informations about its position, direction, amount of nectar and difficulty of extraction. After returning to the nest and unloading nectar, it will become the uncommitted follower which abandoned the food source, the dancer that shares information to recruit nest mate and forages the source, or the forager that exploits food without sharing information. The employed bee will modify its food source, if its nectar amount of modified source exceeds the old one, then it will forget the old and memorize the current solution [38, 39].
3. Unemployed forager: This groups of bees consists of scout bees and onlooker bees. The scout bees search for new food source while the onlooker bees wait for information that will be shared by employed bees. Based on their judgment of its

profitability, the onlooker bees will engage themselves in task of exploiting corresponding food source and become employed bee [38].

The optimization problems are based on the model of cost functions $\mathbf{F}(\mathbf{x})$ which penalize any decision variables \mathbf{x} configuration. Therefore, the following problem is considered for global optimization [15, 39].

$$\min \mathbf{F}(x), \quad \text{for } \mathbf{x} = (x_1, x_2, \dots, x_n) \in \mathfrak{R}^n \quad (2.80)$$

The search space \mathbb{S} is defined as n-dimensional rectangle in \mathfrak{R}^n whose variables is bounded by their upper (u) and lower bound (l).

$$l(i) \leq x(i) \leq u(i), \quad \text{for } 1 \leq i \leq n \quad (2.81)$$

The feasible region of solution $\mathbb{F} \subset \mathbb{S}$ is defined by a set of m additional constraint $m \geq 0$:

$$g_j(i) \leq 0, \quad \text{for } j = 1, \dots, q \quad (2.82)$$

$$h_j(i) = 0, \quad \text{for } j = q + 1, \dots, m. \quad (2.83)$$

Generally, artificial bee colony algorithm consists three types of bees: employed, onlooker, and scout bees. Besides, it has four phases: initialization phase, employed bee phase, onlooker bee phase and scout bee phase.

Initialization phase

In artificial bee colony algorithm, the initial possible solution is randomly generated in range of lower and upper bound of search domain by equation 2.84 [15].

$$x_{i,j} = x_j^{lb} + rand(0, 1) \times (x_j^{lb} - x_j^{ub}), \quad (2.84)$$

where $i \in \{1, \dots, S_n\}$, $j \in \{1, \dots, n\}$, x_j^{lb} and x_j^{ub} are lower and upper bound for j^{th} dimension, respectively.

The amount of nectar for any source, which is the fitness or quality of any possible solution, is given by [15]:

$$fit(\mathbf{x}_i) = \begin{cases} \frac{1}{1 + f(\mathbf{x}_i)}, & \text{if } f(\mathbf{x}_i) \geq 0 \\ 1 + abs(f(\mathbf{x}_i)), & \text{if } f(\mathbf{x}_i) < 0 \end{cases} \quad (2.85)$$

Employed bee phase

The first half of the colony is employed bees whose numbers is equals to number of available food sources around nest. The food source simulate the possible solution of the problems while amount of nectar represent quality or fitness of solution. The employed bee carries both food and necessary information which should be shared with onlookers. The position of food source represents a possible solution for optimization problem. The employed bee whose food source is abandoned by other bees become scout or onlooker bee. On the other hand, the employed bee will modify the food source in its memory based on visual information and tests nectar of a new source. The decision, ether to remember or forget the old source depends on whether its nectar amount is higher or lower than the new source. The employed bee modify the old source position (\mathbf{x}_i) and generate new candidate food position (\mathbf{v}_i) by [15, 40, 41]:

$$v_{i,j} = x_{i,j} + \phi_{i,j}(x_{i,j} - x_{k,j}), \quad (2.86)$$

Where $k \in \{1, \dots, S_n\}$, $j \in \{1, \dots, n\}$ are selected randomly, and $k \neq i$, $\phi_{i,j}$ is any random number in range of $[-1,1]$. As the visual difference between the $x_{i,j}$ and $x_{k,j}$ decrease in front of bee eye, the perturbation on the position(solution) $x_{i,j}$ decrease. Therefore, as the search approaches to optimal solution in searching space (\mathbb{SN}) the step length decreases. Whenever the value of new solution is out of the boundary, it will be set to appropriate solution in the allowed range. Soon after, employed bee chooses the more qualified solution with better fitness value by greedy selection algorithm [40].

Onlooker bee phase

The onlooker bee discovers food source after watching employed bees waggle dance that transmit information about position and nectar amount of available food source. Then the onlooker bee chooses a food source for further exploitation based on its fitness or probability. The probability of food source is calculated by equation 2.87 in [15, 40, 41].

$$P_i = \frac{fit_i}{\sum_{n=1}^{SN} fit_n} \quad (2.87)$$

Each onlooker bees set magnitude of the probability as minimum requirement to choose any food source which is pointed by employed bees waggle dance. Whenever the probability exceed random set point of onlooker bee, it will follow the information given by the employed bee and exploit the food source. Then the onlooker bee generate a candidate solution like employed bee by equation 2.86 and perform greedy selection based on its fitness value [15, 37, 39].

Scout bee phase

The potential bee that has no knowledge about the food source becomes either the scout or onlooker bee. The scout bee explores the environment for new food source. Then the abandoned food source is replaced by a new one which is discovered by scouts. In artificial bee colony algorithm, the solution which is not improved until its trial count exceeds a limit is abandoned source [37, 40].

$$x_{i,j} = x_j^{lb} + rand(0, 1)(x_j^{ub} - x_j^{lb}) \quad (2.88)$$

2.3.2 Drawback of original ABC algorithm

In population based optimization algorithms, the exploration and exploitation performance play significant role. The former refers the ability to investigate various region to discover the new solution space of optimization while exploitation refers to the ability of using the old global best solution information to find a new better candidate root [15, 42]. In artificial bee colony algorithm, the new candidate solution is generated from the randomly selected old one by moving it toward or away from another solution. Therefore, it is random enough for exploration, but the new candidate solution is not promising because it has equal opportunity of being good or bad solution. For this reason, the artificial bee colony algorithm is good in exploration but poor in exploitation [15, 42, 43].

2.3.3 Variants of artificial bee Colony algorithm

Both exploitation and exploration performances are significant in any population based algorithms, but the existence of those two elements by itself does not promise excellent performance unless both are reasonably balanced. The unbalanced nature of this to two factors leads several researchers to develop different search equation to improve its exploitation performance [15, 42, 43].

Gbest-guided artificial bee colony algorithm

The Zhu and Kwong have developed Gbest-guided artificial bee colony algorithm (GABC) by incorporating the global best solution information in search equation of ABC. After including the global best term, they have tried to balance exploration and exploitation performance of the algorithm [15, 42].

$$v_{i,j} = x_{i,j} + \phi_{i,j}(x_{i,j} - x_{k,j}) + \psi_{i,j}(x_{best,j} - x_{i,j}) \quad (2.89)$$

Where: $\psi_{i,j}$ is uniform random number in $[0,C]$;
 $\phi_{i,j}$ is uniform random number.

When $\psi_{i,j}$ is set to zero, the gbest guided artificial bee colony algorithm is similar to the original. Thus, it is necessary to select value of global best coefficient carefully to balance between exploitation and exploration performance [42].

Global best artificial bee colony algorithm for numerical optimization

The population initialization plays significant role in convergence speed of any population based algorithms. At the beginning of algorithm, there is no available information about solution. Therefore, it is a very common practice to use randomly generated values in solution space. Instead of random initialization, the chaotic and opposition based learning methods with sinusoidal iterator are used to generate initial solution to take the advantage of its ergodicity, randomness and irregularity nature in [43]. The sinusoidal iterator is described by equation 2.90.

$$ch_{k+1} = \sin(\pi ch_k) \quad (2.90)$$

Where: K is the preset maximum number of chaotic iteration and

$$ch_k \in (0, 1), \quad k = 0, 1, 2, \dots, K$$

Based on the sinusoidal iterator, Gao and Liu has proposed the following algorithm that can be used for population initialization [44]. Besides, the scout bee can uses it for discovering a new food source [43].

In the [43], mutation strategy of differential equation (DE) algorithm, shown in equation 2.91, is adopted in ABC algorithm to increase its convergence speed.

$$v_i = x_{best} + F(x_{r_1} - x_{r_2}) \quad (2.91)$$

Where r_1, r_2, r_3 and r_4 are mutually exclusive random integers in $\{1, 2, \dots, SN\}$, $i \in \{1, 2, \dots, SN\}$ and $F \in [0, 1]$ is scale factor that control rate of evolution. The search equation of artificial bee colony algorithm is given by:

$$v_{i,j} = x_{best,j} + \phi_{i,j}(x_{r_1,j} - x_{r_2,j}) \quad (2.92)$$

Where index r_1, r_2, r_3 and r_4 are different from base index k and mutually exclusive element of $\{1, 2, \dots, SN\}$. The \mathbf{x}_i is the best solution of recent iteration, $j \in \{1, 2, \dots, SN\}$ is randomly chosen index and the uniform random number $\phi_{i,j} \in [-1, 1]$.

Algorithm 1: Chaotic and opposition-based learning [15]

Data: No iteration $K = 300$, Population SN

```

for  $i = 1 \rightarrow SN$  do
    for  $j = 1$  to  $D$  do
         $ch_{0,j} = rand(0, 1) \in (0, 1);$ 
        for  $k = 1 \rightarrow K$  do
             $ch_{k+1,j} = \sin(\pi ch_k)$ 
        end
    end
     $P_{i,j} = x_{min,j} + ch_{k,j}(x_{max,j} - x_{min,j})$ 
end
for  $i = 1$  to  $SN$  do
    for  $j = 1$  to  $D$  do
         $Q_j = x_{min,j} + x_{max,j} - P_{i,j}$ 
    end
end
Select the best from  $P \cup Q$ 

```

Improved artificial bee colony algorithm (IABC)

Normally, the optimal solution of practical problems is not only depends on global optimal information but also sub-optimal experience of the problem. Therefore, the researcher in IABC has considered the sub-optimal information into search equation of the onlooker bees [15].

$$v_{i,j} = \omega x_{best,j} + c_1 \phi_j (x_{best,j} - x_{i,j} + c_2 \Psi_j (x_{subbest,j} - x_{i,j})) \quad (2.93)$$

Where: ω is the inertia weight to control impact optimal solution;

c_1, c_2 are positive constants;

ϕ_j, Ψ_j are uniform random number in $[-1, 1]$;

$j \in \{1, 2, 3, \dots, SN\}$.

The impact factor controlling variable ω is calculated dynamically by [15]:

$$\omega = \omega_{min} + \frac{\omega_{max} - \omega_{min}}{maxcycle} \times t \quad (2.94)$$

Where ω_{min} and ω_{max} are the upper and lower limit of ω ; t is the current iteration; $maxcycle$ is the maximum number of algorithm iteration.

The chaotic and opposition based learning, which is proposed by Gao and Liu, is used during initialization to enhance the population diversity and quality of the solution. Further more, the algorithm adopt chaotic search operator to update the best solution of current iteration if necessary to heighten global convergence. The chaotic variable ch_{i+1} is generated by:

$$ch_{i+1} = 4 \times ch_i(1 - ch_i), \quad for \ i \in [1, K] \quad (2.95)$$

Where: ch_0 is random number in the interval of $(0, 1)$;
 K is length of chaotic sequence.

The chaotic variable ch_i is mapped to chaotic vector \mathbf{ch}_i in the interval of upper bound (\mathbf{x}_{ub}) and lower bound (\mathbf{x}_{lb}).

$$\mathbf{ch}_i = x_{lb} + ch_i \times (x_{ub} - x_{lb}) \quad (2.96)$$

Ultimately, the new candidate solution \hat{x}_i is generated by:

$$\hat{x}_i = (1 - \lambda) \times x_{best} + \lambda \times \mathbf{ch}_i, \quad for \ i = 1, 2, \dots, K. \quad (2.97)$$

Where λ is a shrink factor that become smaller with increase of evolution generation.

$$\lambda = \frac{maxcycle - t + 1}{maxcycle} \quad (2.98)$$

Unlike those all changes done in improved artificial bee colony algorithm, the scout and employed bees search equation is kept unchanged and remain the same as that of original artificial bee colony algorithm.

2.4 Literature Review of Related Articles

2.4.1 Related research v in regenerative braking

The authors in [4] address the problem of increasing regenerative braking energy for high speed railway vehicle using Bellman-Ford algorithm. The researchers generate regenerative braking speed profile by Bellman-Ford algorithm and compared it with constant

Algorithm 2: IABC algorithm [15]

Input: Number of iteration, population size, trial limit, $\omega_{min}, \omega_{max}, c_1, c_2$

Initialization phase

Initialize population by 2.84

$t \leftarrow 0$

while $t \leq max_iteration$ **do**

Employed bee phase

 Generate candidate solution v_i by 2.86

 Greedy selection b/n v_i and x_i

 Compute fitness value by 2.85 and probability p_i by 2.87

Onlooker bee phase

 Choose solution based on its probability P_i

 Generate a new candidate solution with 2.93 and evaluate it.

 Apply greedy selection between v_i and x_i

Memorize best solution

Scout bee phase

 Determine the abandoned source

 Update abandoned source by 2.84

Chaotic update of Best source

 Chaotic search in x_{best} by 2.95 - 2.98 and update if necessary

$t \leftarrow t + 1$

end

braking rate. Besides, the regeneration efficiency is considered as unity in the aforementioned research. In this thesis, the IABC algorithm is used for optimization. The recent study done in Portland and Chicago trains in [31] shows that the constant regenerative braking efficiency cause 27.39% and 21.54% deviation between modeled regenerative braking energy and practically cultivated energy. Based on their validation test done using data from Chicago, Illinois after calibrating it by nonlinear optimization using data from Portland 1.87% and -2.31% prediction error is obtained [31]. For this reason, the exponential regenerative braking efficiency is used in this thesis.

The researcher Kibrom Tadelle in [5] has investigated the regenerative braking energy performance of Addis Ababa railway vehicle. He has analyzed the magnitude of restored energy for railway vehicle. But in this thesis the problem is addressed using optimization algorithms to enhance magnitude of regenerated energy.

2.4.2 Related research in ABC algorithms

Several researcher are engaged in modifying search equation of bees to improve the exploitation performance of ABC algorithm. As the result, several search equation like global best guided are developed to balance the exploration and exploitation performance. In ABC algorithm, the onlooker bees select and exploit food source if its corresponding probability satisfies their randomly set minimum necessity. The onlooker bee set this lower limit of probability (P_{min}), which is used as the criteria of selection, in range of *zero* to *one*. This intelligence behavior of honey bees is simulated by random number generator in computer program [15, 42, 43].

$$P_{min} = rand(0, 1) \quad (2.99)$$

When the probability of all food sources \mathbf{P}_i is less than \mathbf{P}_{min} , the onlooker bee regenerate new criteria, \mathbf{P}_{min} , for the same solution set. This process of compromising their criteria of selection continue until it fall in range of current food source probability. Such phenomena is frequently seen when the population size is large and the solution become closer to optimum value. If the population of bee is larger, the Equation 2.87 will generate a probability closer to zero. Similarly, when the solution converge to global optimum value, almost all food sources will have nearly the same fitness. As a result, the probability of food sources (\mathbf{P}_i) become closer to the inverse of employed bee population (N_E).

$$P_i = \frac{fit_i}{\sum_{i=1}^{N_E} fit_i} \approx \frac{fit}{N_E \times fit} \approx \frac{1}{N_E} \quad (2.100)$$

Assume the probability of food source has a discrete interval $\Delta P = 1/N_E$, then the probability of generating P_{min} in the interval of $[0, max(P_i)]$ become $1/N_E$. This shows that the onlooker bee will stuck in compromising its criteria until it successfully select at least one food source. In other word, the probability of food source being unexploited or neglected by onlooker bees become as follows:

$$P_{neglect} = 1 - \frac{1}{N_E} = \frac{N_E - 1}{N_E} \geq \frac{1}{N_E} \quad (2.101)$$

In this thesis, the onlooker bees are forced to generate their minimum probability requirement in range of *zero* to the maximum food probability of current iteration. This method of generating onlookers criteria gives the better chance of selecting food source for exploitation.

$$P_{min} = rand(0, Max(P_i)) \quad (2.102)$$

Chapter 3

Case Study

This chapter of thesis focus on developing the mathematical model of Addis Ababa Light Rail Transit System based on the available data and rail road amplitude profile.

3.1 Adhesion Force of AALRT System

The adhesion force of Addis Ababa Light Rail Transient is calculated by equation 2.33. The adhesion coefficient μ_a has non-linear relation with speed of vehicle. The adhesion coefficient as the function of speed is determined based on run down test data by equation 2.35, 2.36 and 2.37. In this thesis, the most recent adhesion coefficient equation, which is formulated by French National Railway, as function of speed (v) in kph is adopted [29].

$$\mu_a(v) = 0.24 \times \frac{8 + 0.1v}{8 + 0.2v} \quad (3.1)$$

Table 3.1: AALRT vehicle parameters for adhesion force calculation[5]

Vehicle mass (kg)	Rated passenger capacity(kg)	Overload passenger capacity (kg)	Gravity(g) (m/s^2)	Elevation (α) ($degree$)
44,000	15,240	19,020	9.81	-

The available wheel rail adhesion force as function of speed (v) in m/s at rated condition for level rail (zero gradient) is calculated by equation 2.33 and 2.39 and its characteristic curve is plotted in figure 3.1.

$$F_a(v, \alpha) = 0.24 \times \left(\frac{8 + 0.1(3.6v)}{8 + 0.2(3.6v)} \right) \times 59240kg \times 9.81m/s^2 \cos(\alpha) \quad (3.2)$$

$$F_a(v, \alpha) = 139.474656 \times \left(\frac{8 + 0.36v}{8 + 0.72v} \right) \cos(\alpha) \text{ } kN \quad (3.3)$$

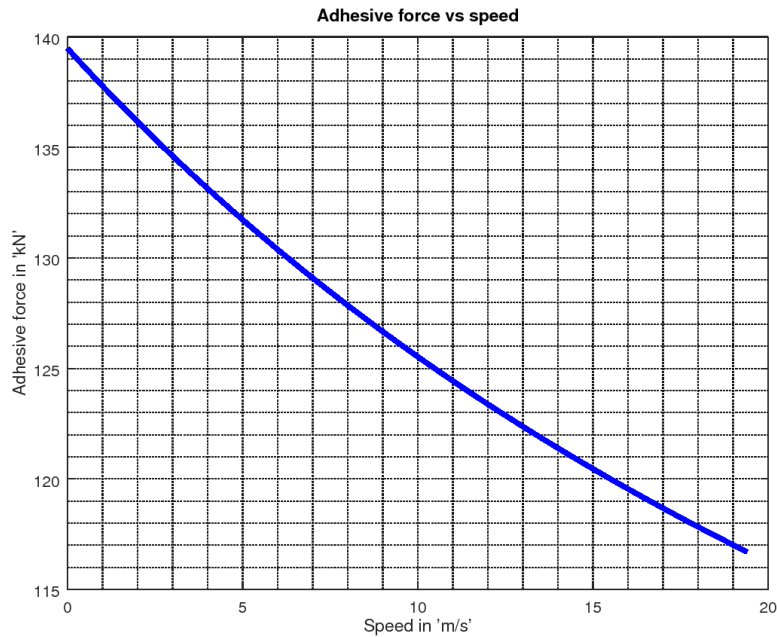


Figure 3.1: Adhesive force vs speed on level railroad

3.2 Grade Resistance of AALRT Vehicle

The grade resistance is the tangential component gravitational force that resists the motion of vehicle as it travel on incline rail. At rated passenger load, the gradient resistance of Addis Ababa light rail transit vehicle is calculated using equation 2.26 and information in table 3.1.

$$F_g(r(s)) = (15,240 \text{ kg} + 44,000 \text{ kg}) \times 9.81 \text{ m/s}^2 \sin(\alpha) \quad (3.4)$$

$$F_g(r(s)) = 581144.4 \sin(\alpha) \text{ N} = 581.1444 \sin(\alpha) \text{ kN} \quad (3.5)$$

The downhill gradient is negative while uphill is positive as train is driven between two consecutive stations. For selected successive inter-station drive, the gradient resistance of AALRT vehicle is calculated using equation 3.5 in table 3.2.

3.3 Running Resistance of AALRT Vehicle

In railway industry, describing the train rolling, bearing, rail-flange and aerodynamic resistance by quadratic function, which is known as Davis equation, is a common practice. But all Davis coefficients are determined based on field test data. On other hand, it can

Table 3.2: Inter-station gradient resistance of AALRT vehicle [5]

No	Stations	Distance [m]	Railroad grade [Degree]	Grade resistance[N]
1	Ayat-2 to Ayat-1	1101	0.00905	91.7931
2	Mazoria to Chemical Co.	920	0.491	4980.0947
3	Meskel square-1 to Legehar	850	2.767	28054.4490

be estimated from the railway vehicle specification in range of 20% uncertainty [17]. In this research, the running resistance coefficient which used for light railway vehicle rolling and aerodynamic resistance in [22] is used.

Table 3.3: AALRT vehicle parameters used for running resistance calculation[5, 6]

Powered bogies	Powerless bogies	Axle per bogie	Rated mass (kg)	C_d
2	1	2	59240	0.07

The mass per axle, w_p , is calculated as follows:

$$w_p = \frac{M_{rated}}{n_p} = \frac{59240 \text{ kg}}{(2 + 1) \times 2} = 9873.33 \text{ kg} = 9.8733 \text{ ton} \quad (3.6)$$

$$R_b(v(t)) = 691.891 + 0.16364v(t) + 0.120108v(t)^2 \text{ N}, \quad [v(t)] = \text{kph} \quad (3.7)$$

$$= 691.891 + 0.58910v(t) + 1.556599v(t)^2 \text{ N}, \quad [v(t)] = \text{m/s} \quad (3.8)$$

3.4 Available Tractive Effort of AALRT Vehicle

The tractive effort of train is the main driving force of railway vehicle which is delivered by the locomotive or engine. In this thesis a point mass model of train is used. Therefore, the total available tractive effort of all engine is summed up as single engine power. The energy transfer coefficient is usually taken as $\eta = 0.7$ [4, 29].

The total power (P_t) which is delivered by the four electric motors of vehicle is

$$P_t = 4 \times 130 \text{ kW} = 520 \text{ kW} \quad (3.9)$$

Therefore, the maximum available tractive effort on level rail is calculated by equation 2.41 and 2.42.

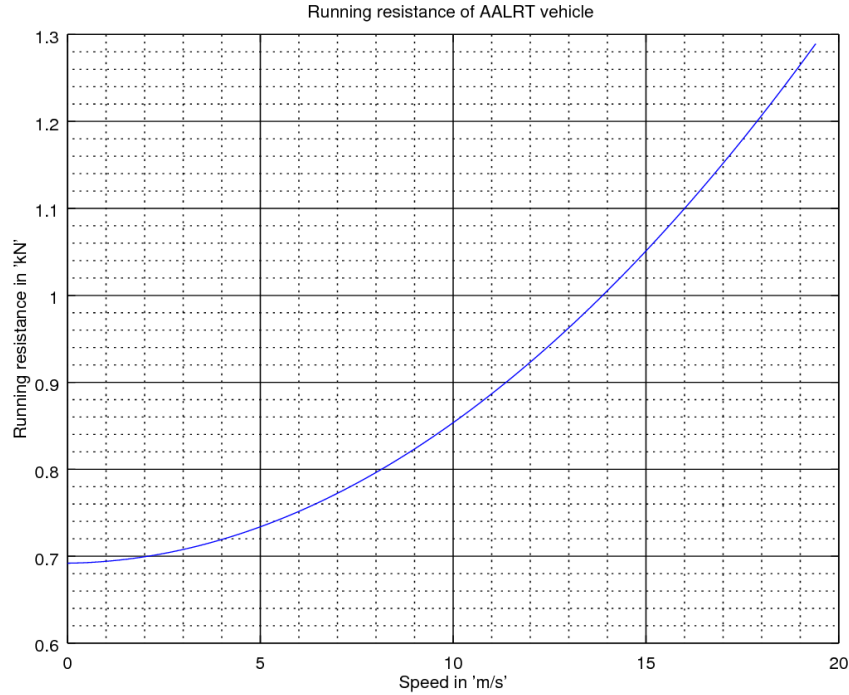


Figure 3.2: AALRT vehicle running resistance vs speed

Table 3.4: AALRT vehicle parameter for tractive force calculation[5, 6]

Number of motors	Power per motor (kW)	Maximum deceleration m/s^2
4	130	1

$$F_{te}^{max}(v) = \frac{0.7 \times 520}{v} \frac{kW}{m/s} = \frac{364}{v} kN \quad (3.10)$$

$$F_{te}(v) = \min(F_{te}^{max}(v), F_a(v, \alpha)) \quad (3.11)$$

3.5 Electrical Braking Force of AALRT Vehicle

Reliable braking operation is one of the critical task that ensure safety and dynamic operations in railway industry. In order to ensure this, the Addis Ababa railway vehicle has the both electrical and mechanical braking system. Even though former restore consumed electrical energy and reduce the mechanical wear out, it cannot stop the train to halt. Therefore, the mechanical braking system is used to halt a train. In this thesis, the regenerative braking operation of railway vehicle is considered and it is assumed that

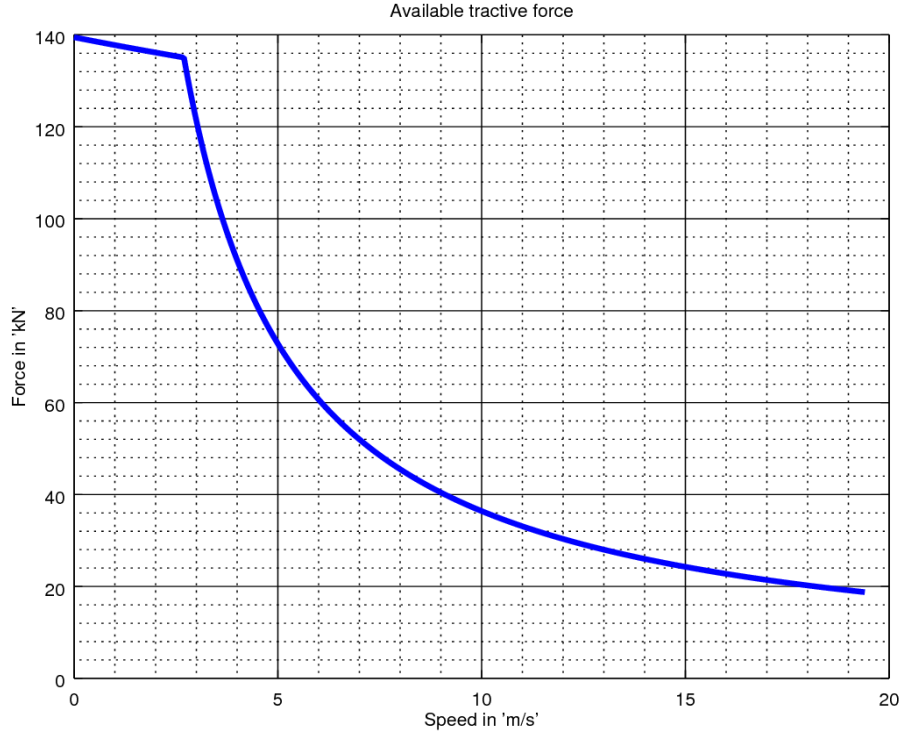


Figure 3.3: The tractive effort of AALRT vehicle with adhesion limit on level rail

the mechanical brake is finally applied to halt a train to stop. The maximum braking deceleration of AALRT is 1 m/s^2 for normal halting operation and 2 m/s^2 for emergency brake [5, 6]. Based on data in table 3.1 the maximum braking force F_{br}^{max} is calculated by equation 2.71 at rated passenger load.

$$F_{br}^{max} = (44,000 \text{ kg} + 15,240 \text{ kg}) \times 1 \text{ m/s}^2 = 59.240 \text{ kN} \quad (3.12)$$

The green shade region of figure 3.4 shows the total regenerable electrical power and the red colored line shows the maximum braking force which should be applied to fulfill deceleration limit. During braking operation, not only the brake effort but also the running resistance oppose the motion of vehicle. Therefore, the magnitude of effective electrical braking force become the difference of total braking force and all resistive forces as described by equation 2.74.

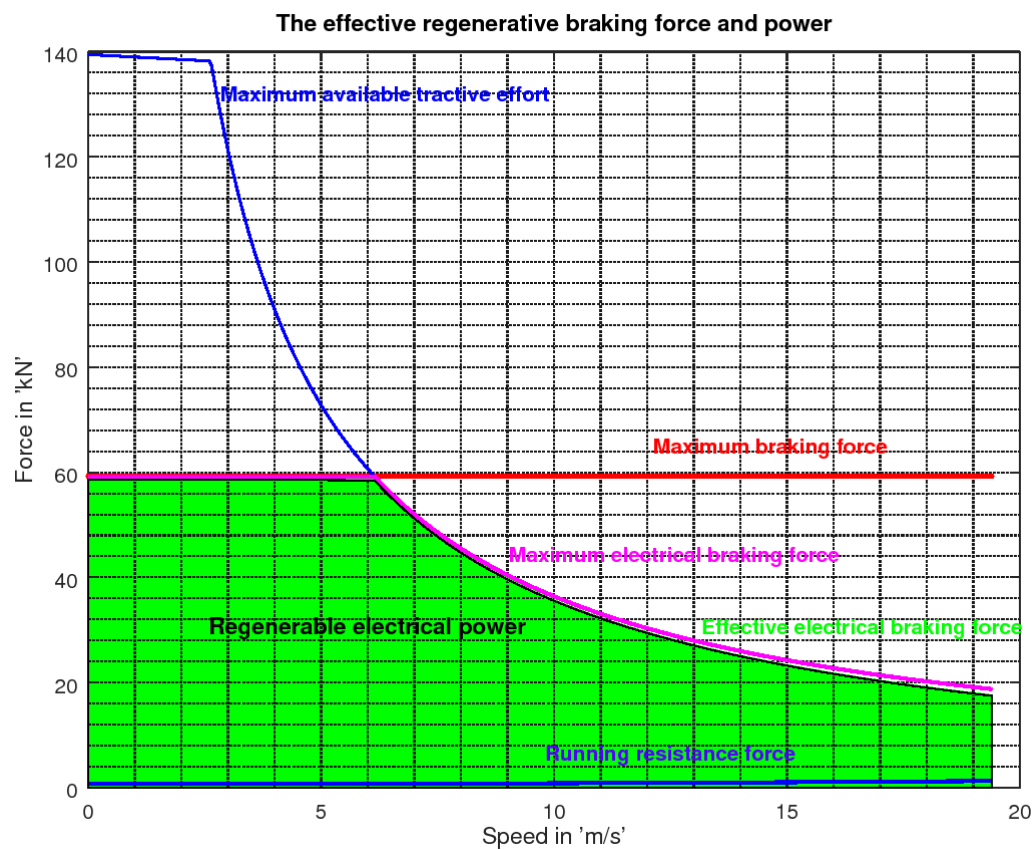


Figure 3.4: Operating range of regenerative braking on level rail

Chapter 4

Results and Discussion

This chapter consists simulation result of a research. In the first section, the maximum regenerative braking energy which is achieved by using IABC algorithm as percentage of kinetic energy is presented. Finally, the recommended speed profile performance is compared with constant braking rate operation in case of Meskel Square-1 and Legehar station.

4.1 The Total Regenerable Electrical Energy

The improved Artificial Bee Colony algorithm is used to search for maximum energy restoration points. The speed profile produced by the artificial bee colony algorithm shows that 1.1984 to 3.3669 MJ energy can be restored by regenerative braking operation. This variation in recovered electrical energy is caused by inter-station railroad grade. The total kinetic energy of vehicle is given by equation 4.1.

$$KE = \frac{1}{2}m_{ef}(v_{max}^2 - 0) = 0.5 \times 59240kg \times (70/3.6)^2 m^2/s^2 = 11.19891975MJ \quad (4.1)$$

The tangential component of gravitational force only resists the uphill traction of vehicle. In downhill braking operation, the tangential component of it has similar direction with velocity of vehicle. In other word, some portion of gravitational potential energy of vehicle is converted to kinetic energy as the train lose its relative height in downhill braking. The kinetic energy due to change in altitude and deceleration from initial speed is then restored to electric power. For this reason, the downhill regenerative braking restores more energy than uphill one as shown in table 4.1.

In figure 4.1 and 4.2, the simulated regenerative braking electric power (in red), which is maximized by IABC algorithm is plotted. Particularly, figure 4.1 shows magnitude of instantaneous power, speed, deceleration and jerk of uphill drive braking in case of Ayat-2 to Ayat-1 station while figure 4.2 shows the reverse direction. As seen from simulation

Table 4.1: Maximized RGBE between Ayat-2 and Ayat-1 station

Direction of motion	Gradient	Restored energy [MJ]		Improvement	Avg RGBP
	[Deg]	CBR	IABC	[%]	[kW]
Ayat-2 \mapsto Ayat-1	0.00905	3.0003	3.2912	29.4083	65.175
Ayat-2 \leftarrow Ayat-1	-0.00905	3.0184	3.2935	29.4286	65.175

result in figure 4.1 and 4.2, its obvious that the optimal speed profile for uphill and downhill drive braking is almost the same for negligibly small rail grade.

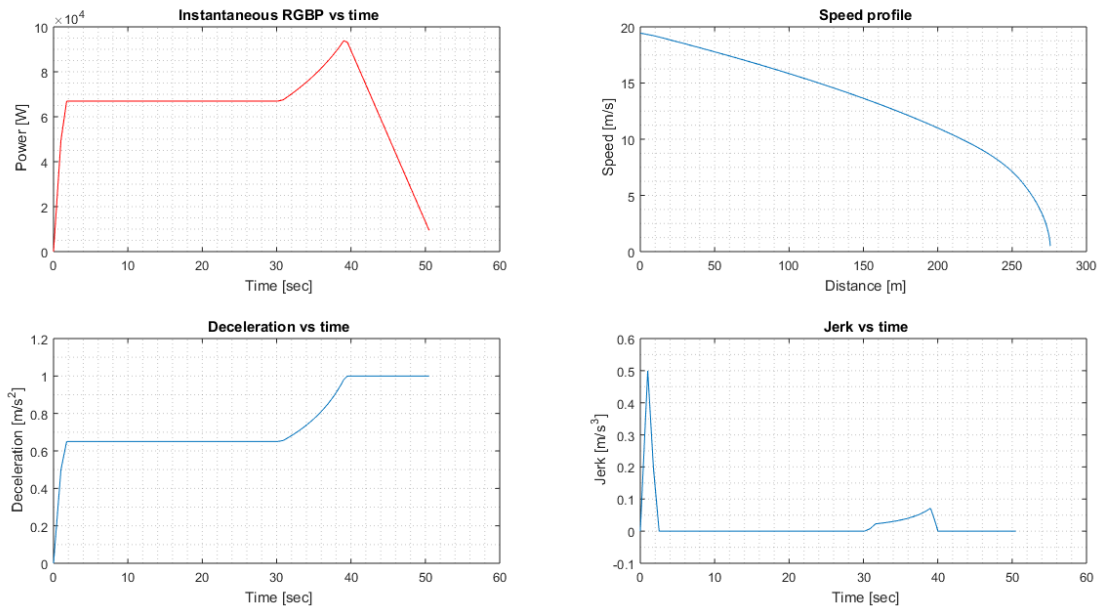


Figure 4.1: Recommended RGB speed profile from Ayat-2 to Ayat-1

Since the train decelerating from maximum speed in still air is assumed, the running resistance, which is independent of rail gradient, is almost the same for different stations. Therefore, the change in regenerative braking energy of different stations is caused by inter-station railroad gradient difference. The simulation results show the increase in steepness of gradient causes significant energy losses due to grade resistance in uphill drive braking operation. This means, significant portion of kinetic energy is converted to potential energy. In contrast, the regenerated energy increase when the rail grade step-up in downhill braking as shown in table 4.1, 4.2 and 4.3.

The simulation result in table 4.2 shows that regenerated energy of downhill drive braking is greater than uphill by following recommended speed profile. Generally as the gradient steepness increases, the uphill drive braking distance and restored energy decrease.

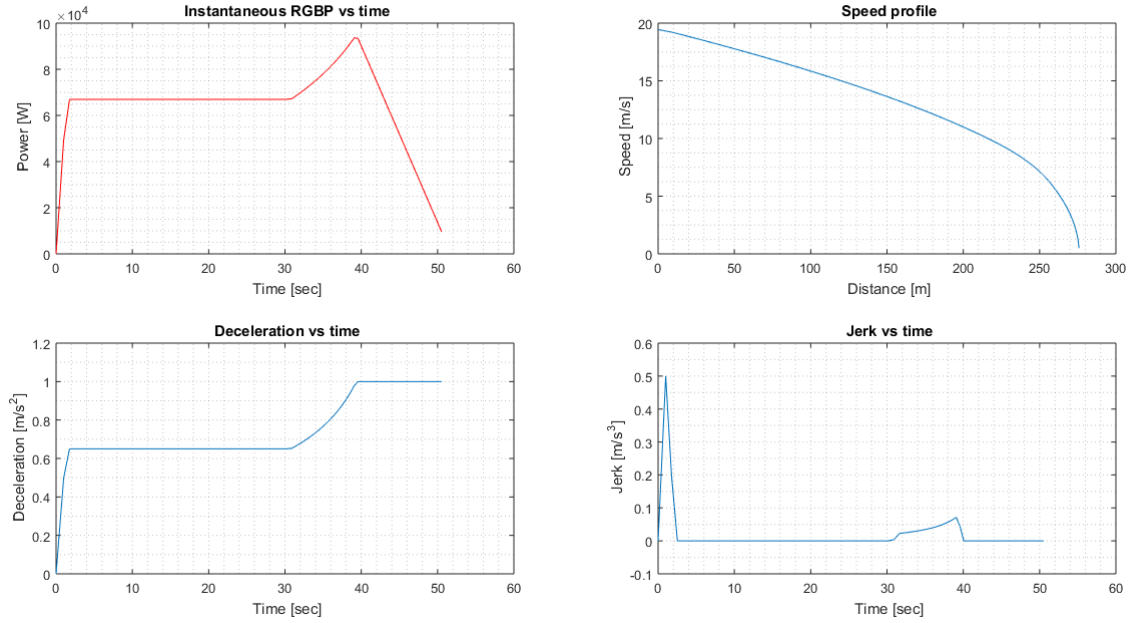


Figure 4.2: Recommended RGB speed profile from Ayat-1 to Ayat-2

Table 4.2: Maximized RGBE between Mazoria & Chemical Co. station

Direction of motion	Gradient	Restored energy [MJ]		Improvement [%]	Avg RGBP [kW]
	[Deg]	CBR	IABC		
Mazoria→Chemical Co.	0.491	2.5183	3.2245	28.8119	65.213
Mazoria←Chemical Co.	-0.491	3.1074	3.3236	29.6976	63.659

When the gradient increase further as seen from Meskel Square-1 to Legehar, the grade resistance causes significant energy loss. But the proposed speed profile restores $1.1984MJ$ energy while $0.6115MJ$ energy is only recovered using constant braking rate (CBR) operation. The maximum speed of a train is achieved when its tractive effort balance all resistive force and no more acceleration is possible. From figure 4.5, it is clearly observed that AALRT vehicle can achieve maximum of $12.5661m/s$ speed and $4.6772MJ$ kinetic energy in case of Meskel Square-1 to Legehar inter-station drive. In downhill braking operation, the gravitational force tend to act as tractive force that accelerate the vehicle, as the result it takes longer time and distance than uphill drive braking as shown in figure 4.5 and 4.6. As seen from simulation result in table 4.3 and 4.4, the proposed method significantly increases regenerative braking energy.

The researchers in [31] shows efficiency of regenerative braking has exponentially increases with magnitude of deceleration. For this reason, the maximum deceleration is selected to simulate constant braking rate speed profile of the railway vehicle. Then

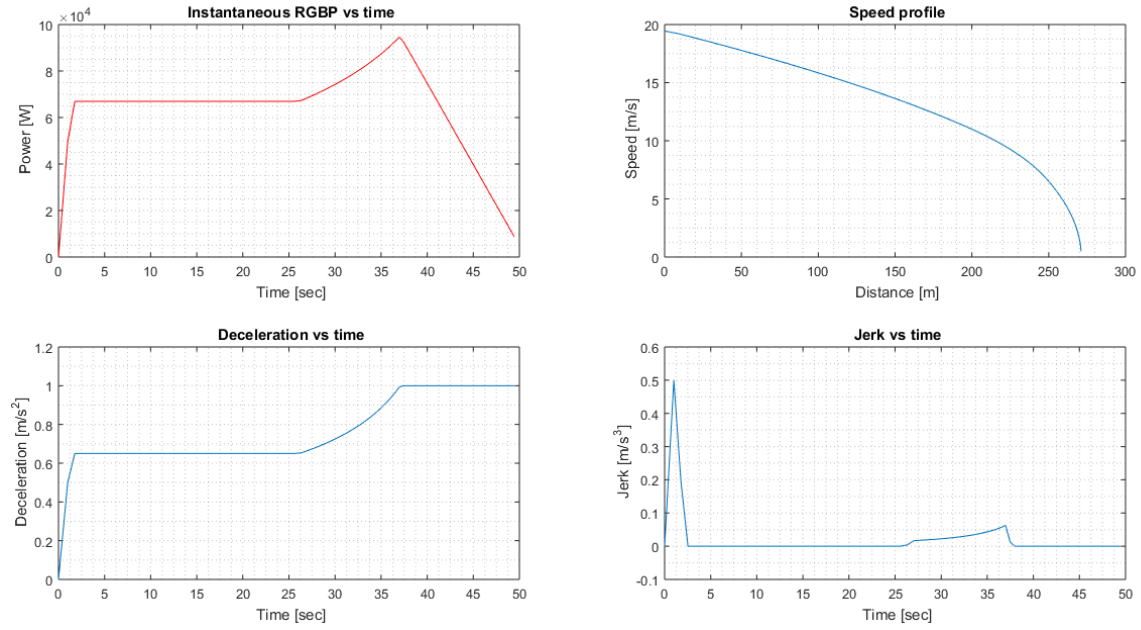


Figure 4.3: Recommended RGB speed profile from Mazoria to Chemical Co.

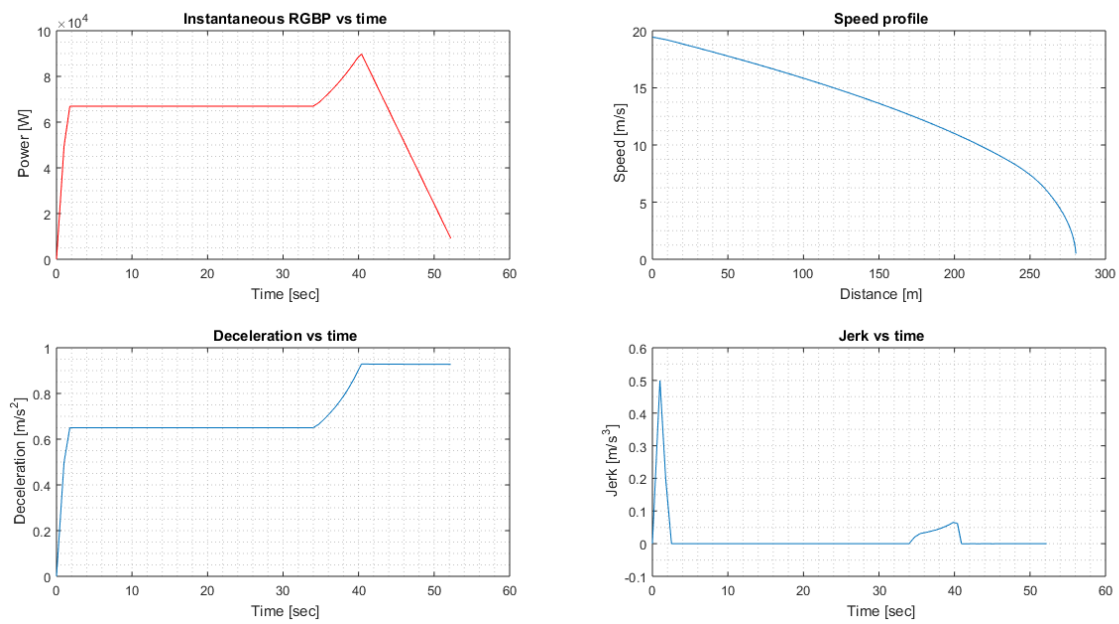


Figure 4.4: Recommended RGB speed profile from Chemical Co. to Mazoria

simulation result of CBR regenerative braking profile is plotted in figure 4.7 and 4.8. Additional simulation results which are not discussed in this chapter are bestowed in appendix A.1.

Table 4.3: Maximized RGBE between Meskel square-1 & Legehar

Direction of motion	Gradient	Restored energy [MJ]		Improvement	Avg RGBP
	[Deg]	CBR	IABC	[%]	[kW]
Meskel S-1 \mapsto Legehar	2.767	0.6115	1.1984	25.6383	47.951
Meskel S-1 \leftarrow Legehar	-2.767	3.1074	3.3669	30.0845	57.528

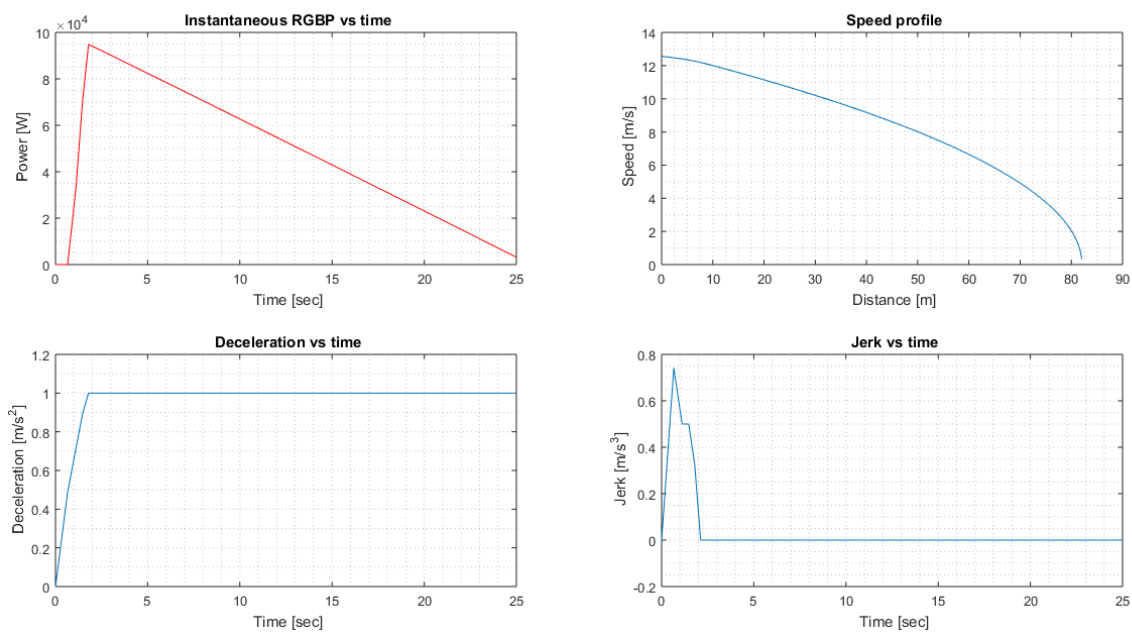


Figure 4.5: Recommended RGB speed profile from Meskel square-1 to Legehar

Table 4.4: Regenerated energy using constant braking rate b/n Meskel square-1 & Legehar

Motion Direction	Grade	Total RGBE	RGBE	Average RGBP
	(Degree)	(MJ)	(%)	(kW)
Meskel S-1 \mapsto Legehar	2.767	0.6115	13.1464	25.093
Meskel S-1 \leftarrow Legehar	-2.767	3.1074	27.7782	82.007

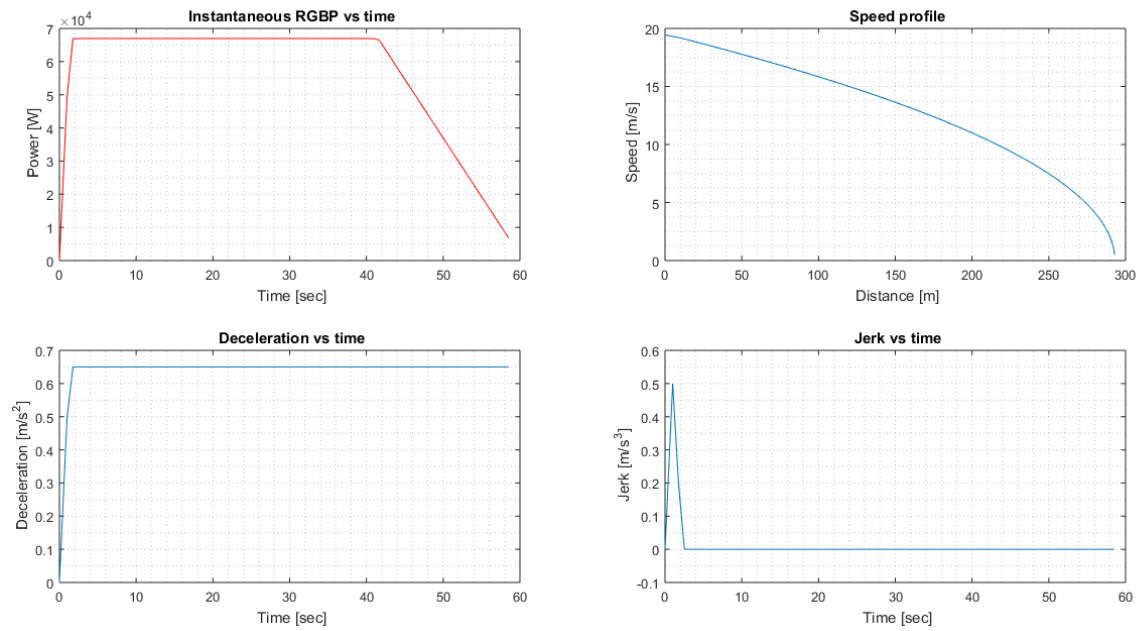


Figure 4.6: Recommended RGB speed profile from Legehar to Meskel square-1

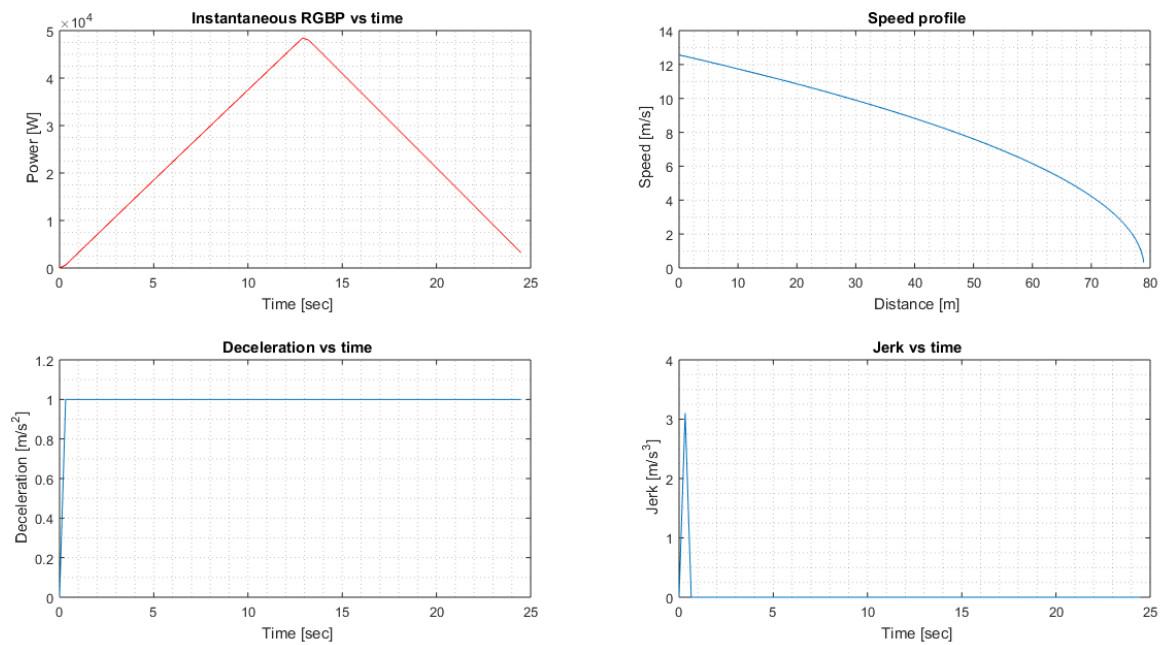


Figure 4.7: Constant braking rate speed profile from Meskel square-1 to Legehar

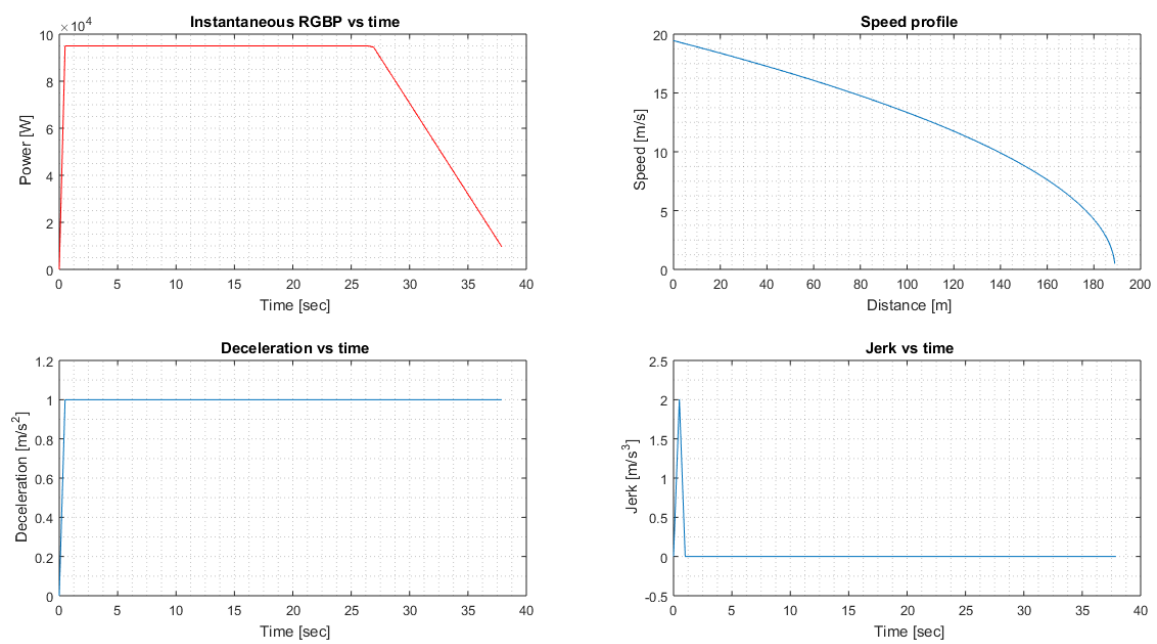


Figure 4.8: Constant braking rate speed profile from Legehar to Meskel square-1

Chapter 5

Conclusion

Analysis of regenerative braking energy is done for selected AALRT stations. Particularly, in case of Ayat-2 and Ayat-1, Mazoria to Chemical corporation and Meskel Square-1 to Legehar stations as it addresses from gentle to steep rail gradient. The simulation result shows the proposed artificial bee colony algorithm based optimization can recover 25.64 – 29.3% of the total kinetic energy in uphill drive braking. Besides, the IABC based optimization regenerate at least 9.11% more electrical energy than traditional constant braking rate operation. Therefore, adherence to recommended braking speed profile of AALRT vehicle has significant factor in maximizing electrical energy restoration. Since running resistance of railway vehicle is independent of rail gradient, the regenerated energy and the speed profile varies with change in inter-station railroad gradient.

5.1 Limitation of The Research

This research is completed under the following limitation:

1. The adhesion coefficient as function of speed is not available for Addis Ababa light rail transit system. Therefore, the adhesion coefficient and speed relation determined by **SNCF** is used to approximate it.
2. The exponential regenerative braking efficiency which is determined by J. Wang and H. A. Rakha based on Portland and Chicago electric train is used [22].
3. Due to lack of available data for determining Davis coefficient of running resistance, the equation proposed by AREA is used in this research.
4. The rotary mass coefficient of train was not available so that it is considered as unity.

Chapter 6

Bibliography

- [1] RailSystem, “Rail gauge.” <http://www.railsystem.net/rail-gauges/>, 2015, Accessed: 11/8/17, 4:10 AM.
- [2] S. Chandra and M. Agarwal, *Railway Engineering*. Oxford University Press, 1st ed., 2007.
- [3] Y. Wang, B. Ning, F. Cao, B. D. Schutter, and T. J. van den Boom, “A survey on optimal trajectory planning for train operations,” *IEEE*, pp. 589 – 594, 2011.
- [4] S. Lu, P. Weston, S. Hillmanssen, H. B. Gooi, and C. Roberts, “Increasing regenerative braking energy for railway vehicles,” *IEEE Transaction on Intelligent Transportation Systems*, 2014.
- [5] T. Kibrom, “Analysis of regenerative braking system in the reduction of energy consumption in addis ababa light rail trains,” msc thesis, School of Mechanical Engineering, 2014.
- [6] B. Mequanint, “Management of regenerative braking energy for addis ababa light rail transit system,” msc thesis, School of Electrical and Computer Engineering, 2014.
- [7] S. Fazel, S. Firouzian, and B. K. Shandiz, “Energy-efficient emplacement of reversible dc traction power substations in urban rail transportation through regenerative energy recovery,” *International Journal of Railway Research*, vol. 1, no. 2, 2014.
- [8] S. Su, T. Tang, and Y. Wang, “Evaluation of strategies to reducing traction energy consumption of metro systems using an optimal train control simulation model,” *Beijing Jiaotong University, State Key Laboratory of Rail Traffic Control and Safety*, 2016.

- [9] P. Zhou and H. Xu, “Train coordinated optimization operation with regenerative braking,” *Journal of Computers*, vol. 7, no. 4, pp. 1025 – 1033, April 2012.
- [10] C. Gong, S. Zhang, F. Zhang, J. Jiang, and X. Wang, “An integrated energy-efficient operation methodology for metro systems based on a real case of shanghai metro line one,” *Energies*, vol. 7, 2014.
- [11] M. Singh, “Regenerative braking: A good source of green energy,” *International Journal of Power Engineering and Energy*, vol. 4, no. 1, pp. 333 – 337, 2013.
- [12] M. Shimida, T. Kaneko, Y. Miyaji, T. Kaneko, and K. Suzuki, “Energy-saving technology for railway traction systems using on-board storage batteries,” *Hitachi Review*, vol. 61, no. 7, pp. 312–318, 2012.
- [13] B. B. Akay and D. Karaboga, “Abc algorithm coded using c programming language.” <http://mf.erciyes.edu.tr/abc/pub/ABC.C>, 2009, Accessed: 26/04/2017.
- [14] S. M. K. Heris, “Implementation of artificial bee colony in matlab.” <http://yarpiz.com/297/ypea114-artificial-bee-colony>, 2015, Accessed 2017.
- [15] C.-F. Wang and Y.-H. Zhang, “An improved artificial bee colony algorithm for solving optimization problems,” *IAENG International Journal of Computer Science*, vol. 43, no. 3, 2016.
- [16] “Step by step procedure of abc.” <https://abc.erciyes.edu.tr/pub/Step%20by%20Step%20Procedure%20of%20ABC.pdf>, 2015.
- [17] G. Boschetti and A. Mariscotti, “The parameters of motion as source of uncertainty for traction system simulation,” *XX IMEKO World Congress Metrology for Green Growth*, 2012.
- [18] Y. Wang, B. D. Schutter, B. Ning, and N. G. T. van den Boom, “Optimal trajectory planning for trains using mixed integer linear programming,” *Proceedings of the 14th International IEEE Conference on Intelligent Transportation Systems*, pp. 1598–1603, 2011.
- [19] B. Rechard and F. Schmid, “A review of methods to measure and calculate train resistance,” *Journal of Rail and Rapid Transit 2000*, vol. 214, no. 185, pp. 185 – 199, Jul 1,2000.
- [20] A. C. . Educational and Training, *Practical Guide To Railway Engineering*. AREA, 2003.

- [21] R. Gawthrop, “Train drag reduction from simple design changes,” *Int. J. of Vehicle Design*, vol. 3, no. 3, pp. 263–274, 1982.
- [22] J. Wang and H. A. Rakha, “Electric train energy consumption modeling,” *Applied Energy* 2017, no. 193, pp. 346 – 355, 2017.
- [23] M. K. Jain, “Train, grade, curve and acceleration resistance.” <https://www.railelectrica.com/traction-mechanics/train-grade-curve-and-acceleration-resistance-2>, 2013, Accessed: 10/22/2017.
- [24] Brown, Boveri, and CO., “Starting diagram of electric train with motors having a series characteristic,” *The Brown Boveri Review*, vol. 10, no. 6, pp. 108 – 115, June 1923.
- [25] Y. Zhu, *Adhesion in the wheel-rail contact*. PhD thesis, Royal Institute of Technology, 2013.
- [26] Y. Zhu, *Adhesion in the wheel-rail contact under contaminated condition*. PhD thesis, Royal Institute of Technology, 2011.
- [27] W. Liao, Y. Song, and W. Cai, “Traction/braking control design for high speed trains based on force estimation- an more implementable approach,” *IEEE*, no. 14, pp. 4437 – 4442, 2014.
- [28] S. Sadr, D. A. Khaburi, and M. Namazi, “A comprehensive model for adhesion control system of wheel and rail,” *Journal of Operation and Automation in Power Engineering*, vol. 5, no. 1, pp. 43–49, 2017.
- [29] K. Kim, *Optimal train control on various track alignment considering speed and schedule adherence constraints*. PhD thesis, New Jersey Institute of Technology, 2010.
- [30] “Tractive effort, acceleration, and braking.” www.m-a.org.uk/TractiveEffortAccelerationAndBraking.doc, 2004 Accessed: Oct 19,2017.
- [31] J.-C. Jong and E.-F. Chang, “Model for estimating energy consumption of electric train,” *Journal of the Eastern Asia Society for Transportation*, vol. 6, pp. 278 – 291, 2005.
- [32] L. Liudvinavicius and L. P. Lingaitis, “Electrodynamic braking in high speed rail transport,” *Transport*, vol. 22, no. 3, pp. 178 – 186, 2007.

- [33] S. Kumar and S. Chaturvedi, “Jerk analysis in rail vehicle dynamics,” *Perspective in science, Elsevier*, no. 8, pp. 648–650, 2016.
- [34] Y.-F. Chang, “Design and implementation of a linear jerk filter for a computerized numerical controller,” *Control Engineering Practice*, vol. 13, no. 2005, pp. 567–576, 2004.
- [35] Wikipedia, “Rail gauge.” [http://www.wikipedia.org/wiki/jerk_\(physics\)](http://www.wikipedia.org/wiki/jerk_(physics)), Nov 24,2017, Accessed: Nov 25,2017, 8:39 PM.
- [36] L. Liudvunavicius and L. P. Lingaitis, “Locomotive energy saving possibility,” *Transport problems*, vol. 4, no. 3, pp. 35–42, 2009.
- [37] D. Karaboga and B. Akay, “A comparative study of artificial bee colony algorithm,” *Applied Mathematics and Computation*, vol. 214, no. 2009, pp. 108–132, 2009.
- [38] D. Karaboga, “An idea based on honey bee swarm for numerical optimization,” 2005.
- [39] D. Karaboga and B. Basturk, “A powerful and efficient algorithm for numerical function optimization: artificial bee colony (abc) algorithm,” *J Glob Optim*, vol. 39, no. 2007, pp. 459–471, 2007.
- [40] D. Karaboga and B. Basturk, “Artificial bee colony (abc) optimization algorithm for solving constrained optimization problems,” *Springer*, pp. 789–798, 2007.
- [41] S. Neelima, N. Satyanarayana, and P. K. Murthy, “A comprehensive survey on variants in artificial bee colony(abc),” *International Journal of Computer Science and Information Technologies*, vol. 7, no. 4, pp. 1684 – 1689, 2016.
- [42] G. Zhu and S. Kwong, “Gbest-guided artificial bee colony algorithm for numerical function optimization,” *Applied Mathematics and Computation*, vol. 217, pp. 3166–3173, 2010.
- [43] W. Gao, S. Liu, and L. Huang, “A global best artificial bee colony algorithm for numerical optimization,” *Journal of Computational and Applied Mathematics*, vol. 236, pp. 2741 – 2753, 2012.
- [44] W. Gao and S. Liu, “A modified artificial bee colony algorithm,” *Computers & Operations Research*, vol. 39, pp. 687 – 697, 2012.

Appendices

Appendix A

A.1 Extra simulation result

As the railway vehicle decelerates from maximum speed at full passenger load to rest with a constant braking rate speed profile is plotted in figure A.1, A.2 A.3 and A.4. The deceleration rate is taken at its maximum allowable value to keep passengers in comfort. The constant braking operation jerk is kept below $2m/s^3$ as allowed for safe passenger travel.

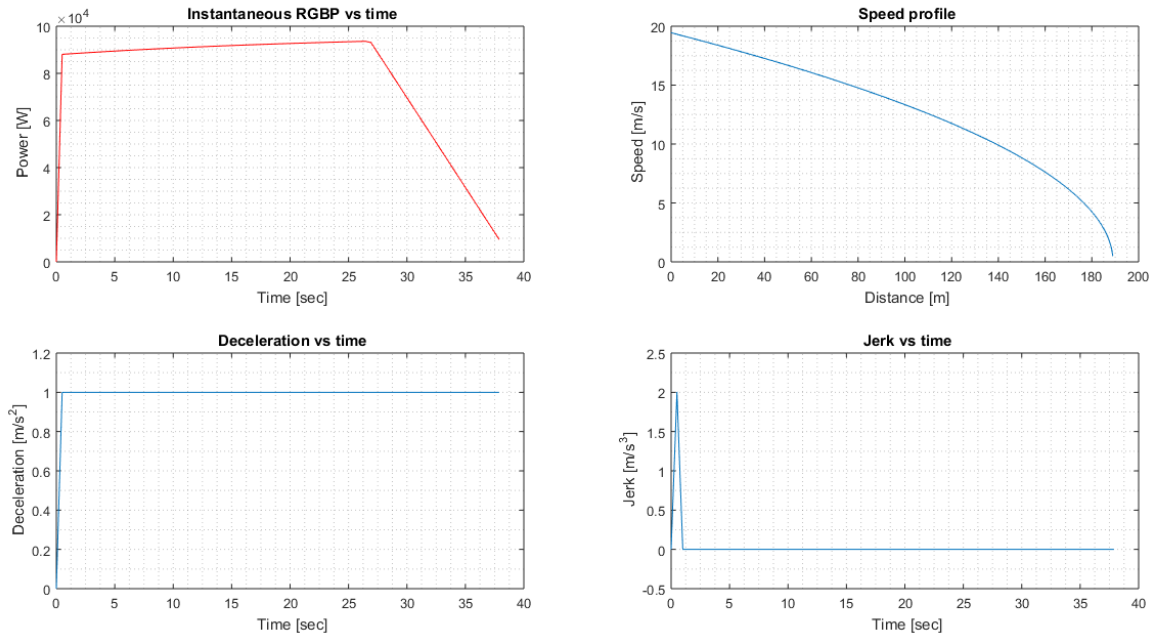


Figure A.1: Constant braking rate speed profile from Ayat-2 to Ayat-1

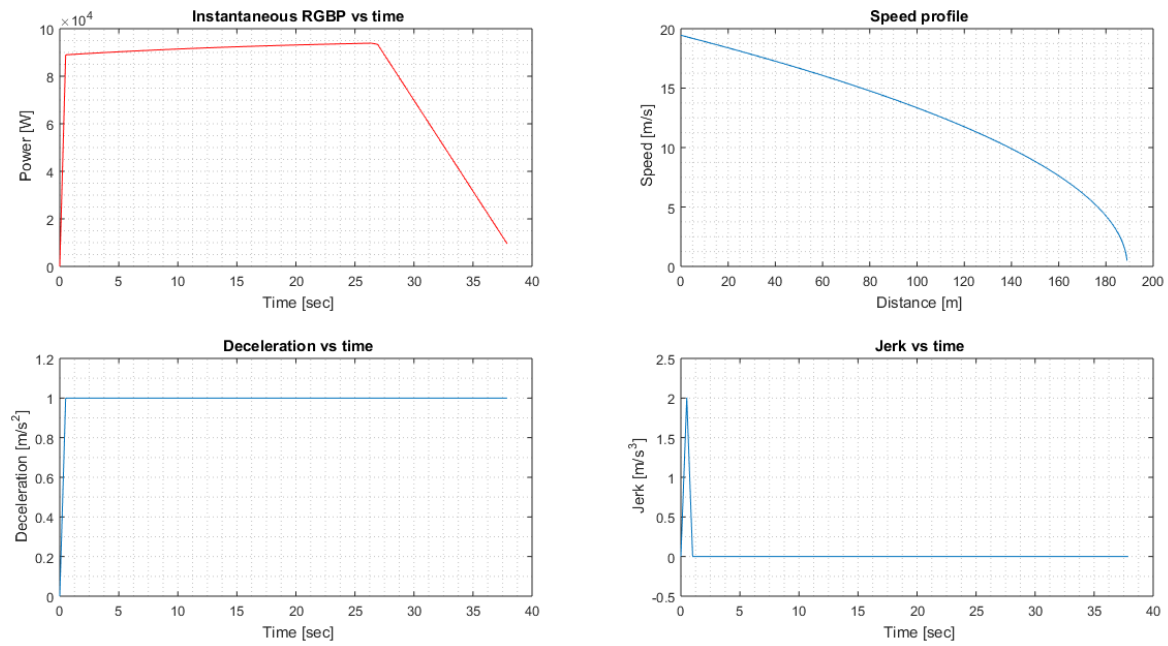


Figure A.2: Constant braking rate speed profile from Ayat-1 to Ayat-2

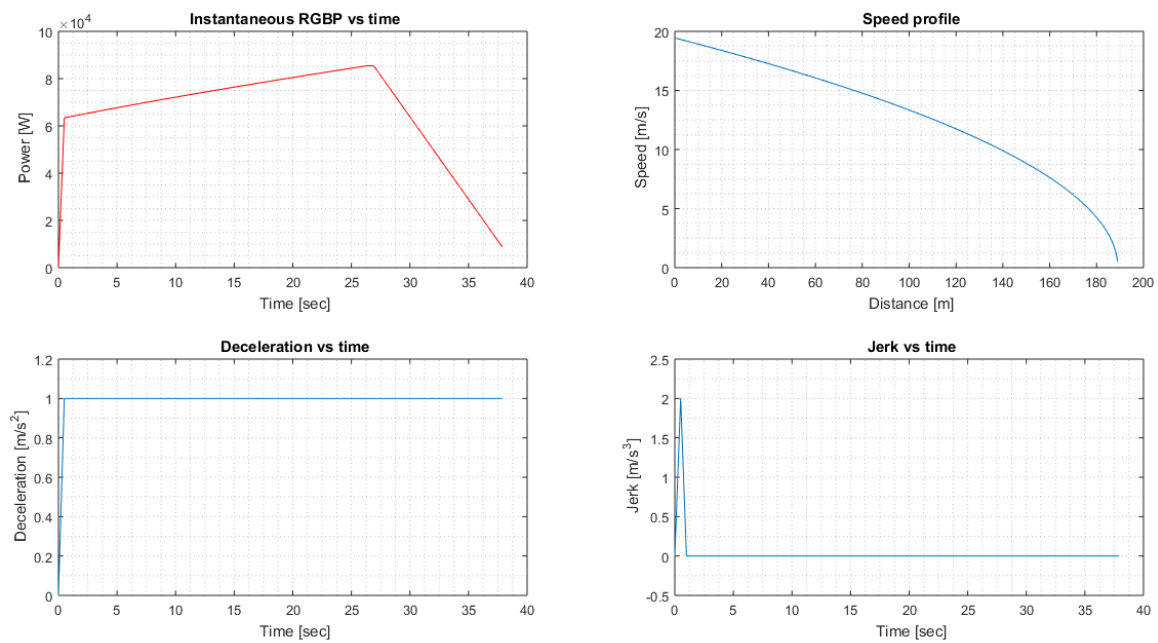


Figure A.3: Constant braking rate speed profile from Mazoria to Chemical Co.

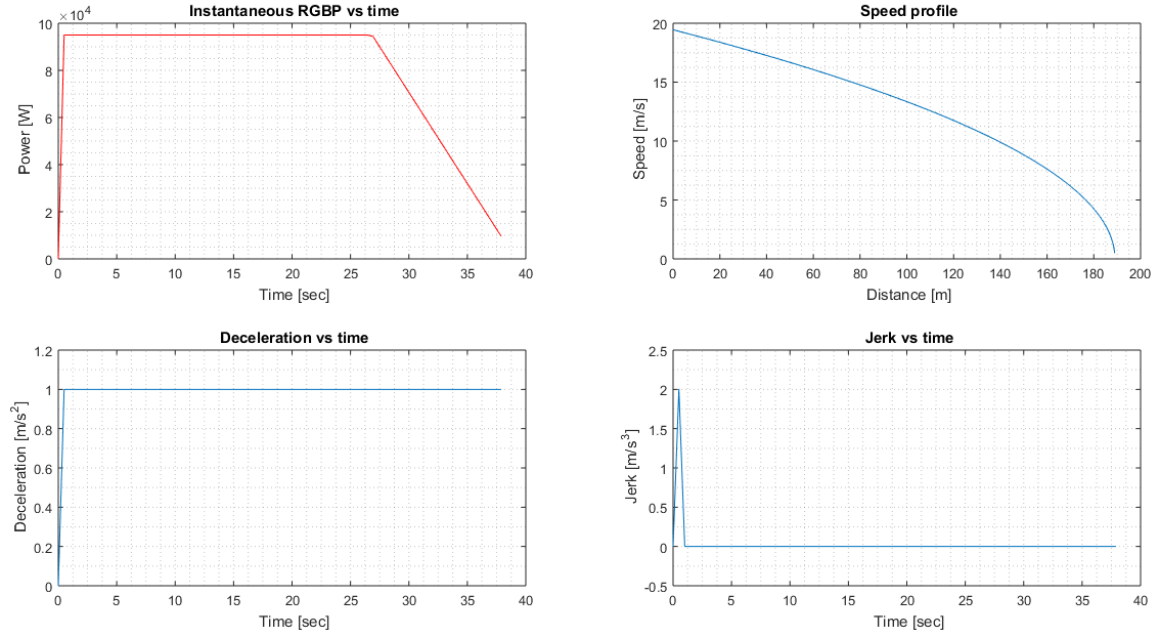


Figure A.4: Constant braking rate speed profile from Chemical Co. to Mazoria

A.2 Addis Ababa LRT gradient profile

In table A.1, the grade resistance is computed as the train travel from Ayat-2 to Tor-hailoch at rated load and at gravity of $9.8m/s^2$. The negative sign indicate the gravitational force is in a direction of drive.

Table A.1: The AALRT rail gradient profile from Ayat-2 to Tor-hayloch [5]

No	Stations	Distance [m]	Gradient [deg]	Gravitational force [N]
1	Ayat-2	1101	0.00905	91.79309
2	Ayat-1	696	0.00818	82.96878
3	CMC-2	758	0.00917	93.01024
4	CMC-1	696	0.00093	9.43288
5	Saint Michael Church	500	0.00958	97.16882
6	Civil service college	506	0.00458	46.45441
7	Sahlite mihret church	673	0.0079	80.12878
8	Gurd shola	565	0.00127	12.88146
9	Meganenga/Adwa square	555	0.00953	96.66167
10	Lem hotel	570	0.00358	36.31152
11	Mazoria/Traffic police HQ	920	0.491	4980.094701

Continued on next page

Table A.1 Continued ...

No	Stations	Distance [m]	Gradient [deg]	Gravitational force [N]
12	Chemical Corporation	740	-1.641	-16642.195
13	Saint Urael church	760	0.00989	100.31311
14	Yordanos Hotel	930	0.00849	86.11307
15	Meskel square-2	952	0.00155	15.72147
16	Meskel square-1	850	2.767	28054.449
17	Leghar	910	1.901	19278.0835
18	Road Authority	725	0.00102	10.34574
19	Mexico square	1005	-1.591	-16135.2534
20	Lideta	660	-2.247	-22785.2168
21	Coca cola	1150	0.00998	101.2259
22	Tor-hailoch	1260	0.00504	51.12013